D8.2
Report on the components of the *in silico* modelling and simulation environment

Project Number: FP6-2005-IST-026996

Deliverable id: ACGT_D8.2_ICCS_final

Deliverable name: Report on the components of the in silico modelling and simulation environment

Submission Date: 15/12/2007

RESTRICTED TO THE ACGT CONSORTIUM AND THE EUROPEAN COMMISSION

COVER AND CONTROL PAGE OF DOCUMENT	
Project Acronym:	ACGT
Project Full Name:	Advancing Clinico-Genomic Clinical Trials on Cancer: Open Grid Services for improving Medical Knowledge Discovery
Document id:	ACGT_D8.2_ICCS_final
Document name:	Report on the components of the *in silico* modelling and simulation environment
Document type (PU, INT, RE)	RE
Version:	1
Submission date:	15/12/2007
Editor: Organisation: Email:	Georgios S. Stamatakos ICCS-NTUA gestam@central.ntua.gr

Document type PU = public, INT = internal, RE = restricted

NB This document is restricted to the ACGT Consortium and the European Commission *until* the standard scientific publication of the contained work.

ABSTRACT:

This report presents the initial version of the simulation component of the ACGT Oncosimulator. The document is also to be used as a complement of the corresponding simulation codes with which it constitutes deliverable D8.2. It provides a description of the medical and basic science problems addressed, an outline of the simulated biological mechanisms and their interdependencies, a brief list of the mathematical concepts and methods recruited or newly developed and applied, an overview of the simulation code, some indicative simulation results and a list of the next developmental steps. The simulation results already obtained substantiate the clinical potential, the flexibility and the robustness of this novel component, especially in view of its expected translation into the clinical environment in order to serve as a patient individualized treatment optimization tool, following a strict prospective clinical validation procedure.

KEYWORD LIST: *in silico* oncology, oncosimulator, cancer, tumour growth, modeling, simulation, therapy response modeling, cancer biology, clinical oncology, cancer treatment, optimization, cellular automata, Monte Carlo, multilevel modeling, multiscale modeling, breast cancer, nephroblastoma, Wilms tumour.

MODIFICATION CONTROL			
Version	Date	Status	Author
1.0	02/12/07	Draft	G. Stamatakos
2.0	07/12/07	Draft	D. Dionysiou
3.0	13/12/07	Draft	N.Graf
4.0	14/12/07	Final	G. Stamatakos

List of Contributors

- Dimitra Dionysiou, ICCS-NTUA
- Eleni Kolokotroni, ICCS-NTUA
- Eleni Georgiadi, ICCS-NTUA and FORTH
- Norbert Graf, USAAR: "*continuous" clinical feedback provider*
- Christine Desmedt, IJB
- Nikoletta Sofra, ICCS-NTUA and Imperial College London
- Persefoni Karvouni, ICCS-NTUA
- Alexander Hoppe, USAAR

Contents

CONTENTS

1 EXECUTIVE SUMMARY....6
2 INTRODUCTION....7
3 THE MEDICAL AND BASIC SCIENCE PROBLEMS ADDRESSED....8
4 AN OUTLINE OF THE SIMULATED MECHANISMS AND THEIR INTERDEPENDENCIES....9
5 MATHEMATICAL CONCEPTS AND METHODS....22
6 AN OVERVIEW OF THE SIMULATION CODE....22
7 INDICATIVE RESULTS....43
8 NEXT STEPS....58
9 CONCLUSION....58

1 Executive Summary

This report presents the initial version of the simulation component of the ACGT Oncosimulator. The module under consideration which includes novel algorithms and computer codes simulates the spatiotemporal course of a solid tumour; in this case of nephroblastoma or breast cancer that is chemotherapeutically treated in the neoadjuvant setting according to protocols dictated by the SIOP 2001/GPOH or the TOP clinical trial respectively. The simulation component aims, after its prospective clinical refinement and validation, and in conjunction with a number of technological complementary components to support the clinician in the selection of the optimal treatment for a given patient, based on his or her imaging, histopathological, molecular and clinical data. The fundamental simulation strategy, the assumptions made, the complexity diagrams developed and a presentation of the basics of the accompanying computer code constitute the core of the document. Indicative simulation results already obtain substantiate the potential, the flexibility and the robustness of the models. A brief outline of the next developmental steps is also provided at the end of the report.

2 Introduction

The aim of the present report is to provide a brief description of the first version of the simulation component of the Oncosimulator as well as some indicative results already obtained with it. A detailed description of the more advanced versions of the simulation component as well as the technological components that together will constitute the Oncosimulator will be given within the framework of future ACGT deliverables and scientific publications according to the currently valid ACGT Description of Work.

The cores of the two current versions of the simulation code corresponding to the two clinical cases considered i.e. nephroblastoma and breast cancer are essentially the same. Their main difference, apart from the different values of the model parameters, lies in the different pharmacokinetics and pharmacodynamics submodules for the drugs/ combinations of the drugs administered. The "D8.2 DEMONSTRATION OF COMPONENTS OF THE *IN SILICO* MODELLING AND SIMULATION ENVIRONMENT - INITIAL SIMULATION COMPONENT OF THE ONCOSIMULATOR: BREAST CANCER VERSION" and "D8.2 DEMONSTRATION OF COMPONENTS OF THE *IN SILICO* MODELLING AND SIMULATION ENVIRONMENT - INITIAL SIMULATION COMPONENT OF THE ONCOSIMULATOR: NEPHROBLASTOMA VERSION" are to serve as the demonstration parts of D8.2.

The simulation models are based on the "top-down" modeling approach developed by the *In Silico* Oncology Group, ICCS, National Technical University of Athens. Their aim is to simulate, within defined limits of reliability, tumour growth and response to pre-operative chemotherapy for the cases of nephroblastoma (Wilms' tumour) and breast cancer. To this end a tight and highly fruitful collaboration with the responsible clinicians has been developed. Cellular automata, the generic Monte Carlo technique and pharmacokinetic differential equations constitute the mathematical basis of the simulation. A discretizing mesh covers the anatomic area of interest. A system of quantizing cell clusters included within each geometrical cell of the discretizing mesh lies at the heart of the simulation approach, as described in detail below. Various mechanisms such as tumour expansion or shrinkage and the effects of particular drugs on the tumour under consideration are incorporated and explicitly described.

The following issues are addressed in the rest of the document:

- the medical and basic science problems tackled
- the simulated biological mechanisms and their interdependencies
- the mathematical concepts and methods recruited or developed and applied
- the simulation code
- indicative results
- the next developmental steps

Finally an overall conclusion appears at the end.

3 The Medical and Basic Science Problems Addressed

In the case of nephroblastoma, the simulation algorithms so far address the cases of preoperative chemotherapy for unilateral stage I-III tumours treated in the framework of the ACGT clinical trials (SIOP 2001/GPOH) with a combination of actinomycin-D and vincristine (see Deliverable 12.1 and Fig. 1). The case of stage IV pre-operative treatment with actinomycin-D, vincristine and doxorubicin will be addressed in future versions of the simulation model.

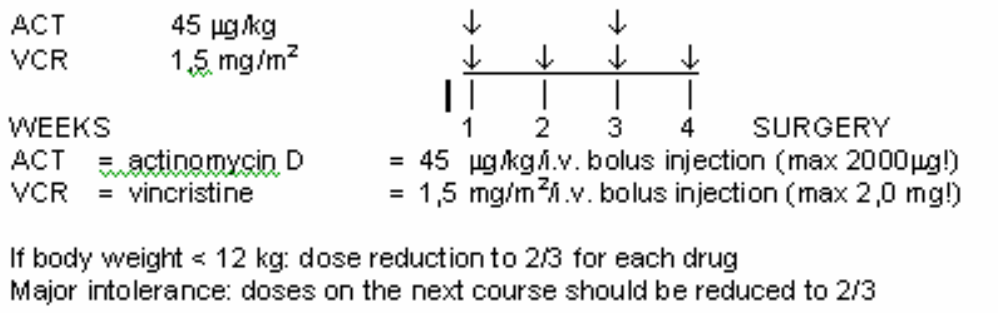

Fig. 1. The simulated therapy protocol for Wilms' tumours. See ACGT Deliverable 12.1.

In the case of breast cancer, the simulation algorithms so far address the cases of primary chemotherapy ("neo-adjuvant" chemotherapy) with single-agent epirubicin (100 mg/m^2 i.v. once every 3 weeks for 4 consecutive cycles) for early breast cancer patients in the framework of the ACGT clinical trials (TOP trial) (see Deliverable 12.1 and Fig. 2).

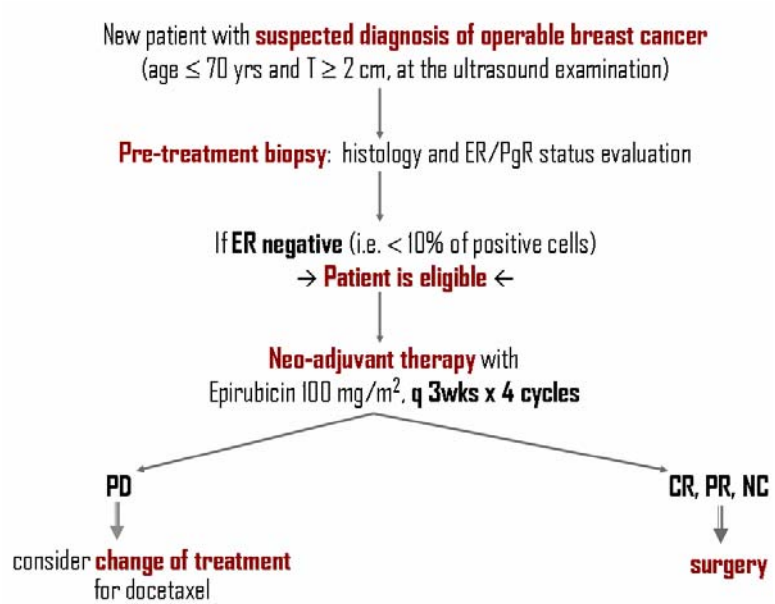

Fig. 2. The simulated therapy protocol for early breast cancer tumours. See ACGT Deliverable 12.1.

As a first approximation, spatially homogeneous tumours of ellipsoidal and spherical shape are considered for nephroblastoma and breast cancer, respectively. This is a reasonable first approximation based on accumulated clinical experience for these tumours and on the fact that the triaxial ellipsoid shape is extensively used in clinical trial case report forms for nephroblastoma, while the maximum diameter of the tumour is used in Case Report Forms for breast cancer.

In fact, nephroblastoma tumour volume is computed in the framework of ACGT clinical trials based on imaging studies as: V=a x b x c x 0.523 cm^3, where a: length (cm), b: width (cm), c: thickness (cm). In a similar manner, the primary chemotherapy response in the case of breast cancer is computed based on ultrasound imaging as: response = (1-size tumour at the end of neo-adjuvant treatment/size tumour at baseline) x100%, where the size of the tumour is defined as the maximum diameter measured by ultrasound imaging data.

The triaxial ellipsoidal shape can produce the special shapes of prolate and oblate spheroids and spheres. More general shapes and non homogeneous internal tumour structures will be addressed in subsequent versions of the simulation code. It should also be noted that the term “homogeneous” tumour in this context refers to the absence of large local differences, such as an obvious necrotic core or an obvious proliferative rim, based on macroscopic imaging data.

4 An Outline of the Simulated Mechanisms and their Interdependencies

SIMULATION OF DRUG PHARMACOKINETICS-PHARMACODYNAMICS

A thorough study of the pharmacokinetic and pharmacodynamic characteristics of the involved chemotherapeutic agents (actinomycin-D and vincristine for the case of Wilms’ tumour and epirubicin for the case of breast cancer) has been conducted. Details of the simulation approach adopted for each case are presented in the following paragraphs.

It should be noted that for any drug there are numerous sources of interpatient variability concerning both pharmacokinetics and pharmacodynamics. Appropriate adjustment of the various related parameters according to clinical data which will be provided in the framework of ACGT trials is facilitated by the discrete nature of the model and is expected to satisfactorily reflect this variability. Therefore, the pharmacokinetic and pharmacodynamic considerations described below represent typical cases to start with and serve as an indication of the potential of the “Oncosimulator”.

A. Chemotherapeutic agents for the treatment of Wilms’ tumours

A1. Vincristine pharmacokinetics-pharmacodynamics

After a 1.5 mg/m^2 intravenous bolus injection the AUC of vincristine is given in (Groninger et al, 2002) as equal to 6.7mg/L/min.

In (Dahl et al, 1976) an experiment was carried out to test whether the arrest in metaphase of cervical carcinoma cells after treatment with various concentrations of vincristine for 6 hours was reversible. Treatment with 16×10^{-3} ug/ml of vincristine for 6 hours seems to produce an irreversible metaphase arrest and an AUC of 5.76 ug/ml/min =5.76 mg/L/min which is very close to the clinical AUC that has been observed in (Groninger et al, 2002). The metaphase index calculated at 90min after the removal of the drug (a time period during which it increases) was equal to 240 (cells stuck in metaphase per 1000 cells). This value of 240/1000=0.24 can be considered to reflect the cell kill fraction in the experiment, since mitosis cannot be completed, the cell cycle cannot proceed and death should follow.

Since the value of 5.76 ug/ml/min for the AUC in this experiment is slightly lower than the clinical AUC value of 6.7 mg/L/min, a cell kill fraction equal to 0.3 could be justified as an initial gross approximation, which is expected to be corrected if necessary with the help of real ACGT clinical data. As a first approximation also, the imperfect drug penetration into the tumour is assumed to have been taken into account in this value of 0.3 cell kill fraction.

The antineoplastic effect of vincristine is basically attributed to its ability to destroy the functionality of cell microtubules, which form the mitotic spindle, by binding to the protein tubulin (Beck et al, 2000). Failure of the mitotic spindle results in apoptotic cell death at mitosis (Wood et al, 2001).

Vincristine is characterised as a cell cycle specific agent (exerts action on cells traversing the cell cycle) (Salmon and Sartorelli, 2001) and more specifically as an M-phase specific drug (Beck et al, 2000), (Pickerton, 1988). Therefore, in the simulation model vincristine is assumed to bind at cells at all cycling phases and lead to apoptotic cell death at the end of M phase.

It should be noted that vincristine cytotoxicity is known to decrease with increasing tumour cell density (“inoculum effect”) (Kobayashi et al, 1998).

A2. Actinomycin-D (Dactinomycin) Pharmacodynamics - Pharmacokinetics

Actinomycin-D is a cell cycle-nonspecific antitumour antibiotic that binds to double-stranded DNA through intercalation between adjacent guanine-cytosine base pairs (Salmon and Sartorelli, 2001), thereby inhibiting its synthesis and function. It also acts to form toxic oxygen-free radicals, which create DNA strand breaks, inhibiting DNA synthesis and function. In the simulation model actinomycin-D is assumed to bind to cells at all cycling phases and lead to apoptosis at end of S phase.

Since recent literature data for dactinomycin pharmacokinetics proved to be rather scarce, a more simplistic approach has been adopted in this case as a first approximation. A cell kill fraction equal to 0.2 has been adopted as a starting point based on the fact that actinomycin-D is considered a less potent cytotoxic drug compared to vincristine, as indicated by lower AUC and higher IC_{50} values for various tumour and normal cells (Sawada et al, 2005, Veal et al, 2005). Imperfect drug penetration into the tumour is assumed to have been taken into account when considering this cell kill fraction value.

A3. Vincristine and Actinomycin-D combined treatment.

According to the SIOP clinical trial protocol, vincristine i.v. bolus injection is directly followed by an i.v. bolus injection of actinomycin-D, with no delay in-between. Therefore, as a first approximation an additive drug effect of vincristine and actinomycin-D has been assumed.

This is considered an optimal starting point for simulating the effect of practically concurrently administered drugs. The corresponding cell kill fractions computed according to the pharmacodynamics of each drug are added in order to acquire the total cell kill fraction (cell kill fraction = 1-cell survival fraction) *[http://www.medscape.com/viewarticle/429259]*, (Scripture and Figg, 2006).

B. Breast cancer chemotherapeutic agent: Epirubicin

B1. Epirubicin pharmacokinetics

Epirubicin pharmacokinetics has been described in various studies by an open three-compartment model. Thereby, an equation for the area under curve, AUC as a function of the dose, the volume of distribution and the transfer rate constants is derived (see Appendix 1).

Typical values for the volume of distribution ($Vd=480.1L/m^2$) and clearance ($CL=74.4L/(hm^2)$) for a dose of 90 mg/m^2 have been derived from (Danesi et al, 2002). Based on these values the elimination constant k_{el}= CL/Vd can be calculated as $0.1555h^{-1}$ and substituted in the equations. For the determination of the transfer rate constants the SAAM II software tool was used [http://depts.washington.edu/saam2/] with the previous input values for Vd, CL and dose as well as the experimental data of plasma concentration versus time to be used by the software for the fitting of the three-compartment model. This leads to an estimation of the transfer rate constants ($k_{12}=0.1498h^{-1}$, $k_{21}=0.7231h^{-1}$, $k_{13}=0.1498h^{-1}$, $k_{31}=0.7231h^{-1}$) and finally permits an estimation of the AUC for any given dose.

B2. Epirubicin pharmacodynamics.

Epirubicin is an anthracycline chemotherapeutic agent, derivative of doxorubicin. It exerts its cytotoxic action through various mechanisms; the most established one is intercalation between bases of double stranded DNA thereby inhibiting DNA synthesis and function. It interferes with DNA transcription and inhibits topoisomerase II by forming a complex with DNA and topoisomerase II, which leads to DNA strand breaks. It also acts to form toxic oxygen-free radicals, causing DNA strand breaks, and inhibiting DNA synthesis and function (Perry, 2008). Epirubicin is considered a cell cycle non-specific drug (Salmon and Sartorelli, 2001). In the simulation model tumour cells are assumed to absorb the drug at all cycling phases and apoptotic death occurs at the end of S phase.

As a first approximation, the survival fraction for epirubicin is computed on the basis of experimental FDA data concerning the pharmacodynamics of epirubicin, and more specifically the *in vitro* cytotoxicity of epirubicin on HeLa cells *[http://www.fda.gov/cder/foi/nda/99/50-778_Ellence_pharmr.pdf]*, as depicted in Table 1 and Fig. 3.

Therefore, the survival fraction can be calculated from the above data by linear interpolation. In this case also, a fraction of the calculated AUC (e.g. 2AUC/3) is a reasonable approximation that may be used to account for inadequate drug penetration into the entire tumour. Particularly for human breast cancer steep doxorubicin gradients have been shown in relevant studies (Lankelma et al, 1999).

Table 1. Experimental data for HeLa cells' survival

Concentration(ug/ml)	Time(h)	AUC	SF
0,125	2	0,25	0,78
0,25	2	0,5	0,66
0,5	2	1	0,6
0,25	8	2	0,54
0,5	8	4	0,47
0,25	24	6	0,4
0,5	24	12	0,34

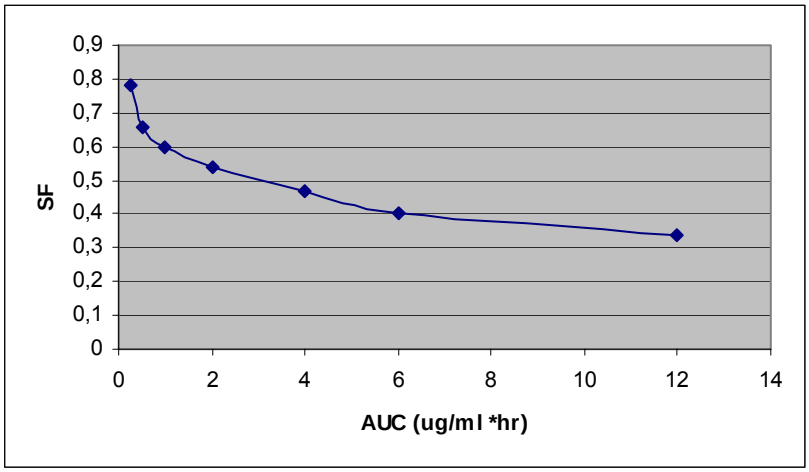

Fig. 3. Experimental data for HeLa cells survival as a function of epirubicin AUC.

Summarizing, for the simulation of primary chemotherapy treatment of early breast cancer patients in the framework of ACGT clinical trial, the following typical parameter values (directly derived from literature or calculated) may serve as a starting basis (Table 2):

Table 2. Typical parameter values adopted in the simulation model for epirubicin pharmacokinetics-pharmacodynamics

Dose (D)	100 mg/m^2

Volume of distribution (Vd)	480.1L/m^2
Inter-compartmental	k_{12}=0.1498, k_{21}=0.7231
transfer rate constants	k_{13}=0.1498, k_{31}=0.7231
Elimination rate constant (k_{el})	0.155
Area Under Curve (AUC)	2/3*0.8877mg*h/L≈ 0.592mg*h/L
Survival fraction	≈ 0.65

PHARMACOKINETICS AND PHARMACODYNAMICS REFERENCES

W.T.Beck, C.E.Cass, P.J.Houghton. Microtubule-targeting anticancer drugs derived from plants and microbes: Vinca alkaloids, taxanes and epothilones. In: Holland JF, Frei E III, Bast RC Jr, Kufe DW, Morton DL, Weichselbaum RR, eds. Cancer Medicine, 5th Edition. Atlanta: American Cancer Society; 2000:680-698.

W.N. Dahl, R. Oftebro, E.O.Pettersen, T. Brustad. Inhibitory and cytotoxic effects of Oncovin (Vincristine Sulfate) on cells of human line NHIK 3025. Cancer Res. 36, 3101-3105, 1976.

R.Danesi, F.Innocenti, S.Fogli, A.Gennari, E.Baldini, A.Di Paolo, B.Salvadori, G.Bocci, P.F.Conte and M.Del Tacca, "Pharmacokinetics and pharmacodynamics of combination chemotherapy with paclitaxel and epirubicin in breast cancer patients", Journal of Clinical Pharmacology, vol. 53, pp 508-518, 2002.

H.Eichholtz-Wirth, "Dependence of the cytostatic effect of adriamycin on drug concenration and exposure time in vitro," Br. J. Cancer, vol. 41, pp. 886–891, 1980.

E. Groninger, T. Meeuwsen-de Boer, P. Koopmans, D. Uges, W. Sluiter, A. Veerman, W. Kamps, S. de Graaf. Pharmacokinetics of Vincristine Monotherapy in Childhood Acute Lymphoblastic Leukemia. Pediatric Research 52: 113-118, 2002.

W.J.Jusko, "Pharmacodynamics of chemotherapeutic effects: Dose-time- response relationships for phase-nonspecific agents," J. Pharm. Sci., vol. 60, no. 6, pp. 892–895, 1971.

H. Kobayashi, Y.Takemura, JF. Holland, T.Ohnuma. Vincristine saturation of cellular binding sites and its cytotoxic activity in human lymphoblastic leukaemia cells. Biochem. Pharmacol. 55: 1229-1234, 1998.

J.Lankelma, H.Dekker, R.F. Luque, S.Luykx, K.Hoekman, P.van der Valk, P.J.van Diest, H.M.Pinedo. Doxorubicin gradients in human breast cancer. Clin Cancer Res 5: 1703-1707, 1999.

A.L.Minchinton and I.F.Tannock. Drug penetration in solid tumors. Nat Rev Cancer 6: 583-592, 2006.

M.C.Perry ed. The Chemotherapy Source Book. USA, Philadelphia: Lippincott Williams & Wilkins, 2008.

C. R. Pinkerton, B. McDermott, T. Philip, P. Biron, C. Ardiet, H. Vandenberg, and M. Brunat-Mentigny Continuous vincristine infusion as part of a high dose chemoradiotherapy regimen: drug kinetics and toxicity, Cancer Chemother Pharmacol 22: 271-274, 1988.

J.Robert. Use of pharmacokinetic-pharmacodynamics relationships in the development of new anthracyclines. Cancer Chemother Pharmacol 32: 99-102, 1993.

S.E.Salmon and A.C.Sartorelli "Cancer Chemotherapy", in Basic & Clinical Pharmacology, B.G.Katzung, ed. Lange Medical Books/McGraw-Hill, International Edition, pp.923-1044, 2001.

K.Sawada, K.Noda, H. Nakajima, N. Shimbara, Y.Furuichi, M. Sugimoto. Differential cytotoxicity of anticancer agents in pre- and post-immortal lymphoblastoid cell lines. Biol Pharm Bull 28: 1202-1207, 2005.

C.D.Scripture and W.D.Figg. Drug interactions in cancer therapy. Nat Rev Cancer 6: 546-558, 2006.

H. E. Skipper, F. M. Schabel, L. B. Mellett, J. A. Montgomery, L. J. Wilkoff, H. H. Lloyd, and R. W. Brockman, "Implications of biochemical, cytokinetic, pharmacologic, and toxicologic relationships in the design of optimal therapeutic schedules," Cancer Chemother. 54: 431–450, 1970.

G.J.Veal, M. Cole, J.Errington, A.Parry, J.Hale, A.D.J.Pearson, K.Howe, J.C.Chiholm, C.Beane, B.Brennan, F.Waters, A.Glaser, S.Hemsworth, H. McDowell, Y.Wright, K.ritchard-Jones, R.Pinkerton, G.Jenner, J.Nikolson, A.M.Elsworth, A.V.Boddy, and UKCCSG Pharmacology Working Groups. Pharmacokinetics of Dactinomycin in a pediatric patient population: a United Kingdom Children's Cancer Study group study. Clin Cancer Res 11(16): 5893-5899, 2005.

K.W.Wood, W.D.Cornwell, J.R.Jackson. Past and future of the mitotic spindle as an oncology target. Current Opinion in Pharmacology 1(4): 370-377, 2001.

OUTLINE OF THE SIMULATION ALGORITHMS

The equivalence classes

Each geometrical cell (GC) of the discretizing mesh constituting the region of interest contains a number of cells (NBC). The typical cell density of 10^9cells/cm^3 (G.Steel, ed. Basic Clinical Radiobiology. London, UK: Arnold, 2002, p.9)) is adopted and therefore a GC of 1mm^3 is assumed to contain 10^6 cells. Each GC includes the following equivalence classes:

- Stem cells: cells assumed to possess unlimited proliferative potential
- Limp cells: cells with **li**mited **m**itotic (proliferative) potential also known as progenitor cells
- Diff cells: terminally **diff**erentiated cells
- Necrotic cells: cells that have died through necrosis
- Apoptotic cells: cells that have died through apoptosis

Stem or limp cells can be proliferating or dormant (G_0) (due to inadequate oxygen and/or nutrient supply). Proliferating stem or limp cells are further distributed into classes corresponding to the cell cycle phase in which they reside: G_1 (Gap 1 phase), S (DNA synthesis phase), G_2 (Gap 2 phase), M (Mitosis). The initial distribution of the proliferating cells to the various cell cycle phases is currently assumed analogous to the corresponding typical cell cycle phase durations, as indicated for malignant cells in the relevant literature (S.E.Salmon and A.C.Sartorelli “Cancer Chemotherapy”, in Basic & Clinical Pharmacology, B.G.Katzung, ed. Lange Medical Books/McGraw-Hill, International Edition, pp.923-1044, 2001):

$$T_{G1} \approx T_C \cdot 40\% \text{ , } T_S \approx T_C \cdot 39\%, \; T_{G2} \approx T_C \cdot 19\%, \; T_M \approx T_C \cdot 2\%$$

Obviously, various initial cell cycle phase distributions can be easily considered.

All cells of a given class within a GC are assumed to be synchronized, whereas cells of different GCs or different classes of the same GC are not synchronized (a random number generator is used for this purpose).

Cytokinetic models for tumour growth and tumour response to chemotherapy

All cells in all GCs follow the cytokinetic diagrams (stochastic cellular automata models) presented in Fig. 4 (for the case of chemotherapy) and Fig. 5 (for the case of untreated tumour growth). These are general cytokinetic models that can be adapted for specific tumour data and drugs under consideration by adequately adjusting the corresponding simulation parameters (e.g. the probabilities of the various transitions between phases, the cell cycle durations etc.).

The biological phenomena incorporated into the simulation models as described in figures 4 and 5 are:

- Cycling of proliferating cells through the subsequent phases of the cell cycle.
- Symmetric and asymmetric stem cell division.
- Proliferation of limited proliferative potential (progenitor) cells (up to n=3 divisions in the current version of the simulation code).
- Terminal differentiation of progenitor cells.
- Spontaneous apoptosis.
- Transition to a dormant (G_0) phase due to inadequate supply with oxygen and nutrients.
- Local reoxygenation and nutrient provision reestablishment.
- Cell death through necrosis due to prolonged oxygen and nutrients deprivation.

- Chemotherapy-induced cell death: possibility of consideration of cell cycle–specific or cell cycle-nonspecific chemotherapeutic agents. Possibility of consideration of distinct cytotoxic mechanisms of drugs, by varying the relative weights of cell death from each cell cycle phase (cell cycle phase-specific drugs) or the phase of the cell cycle in which the drug's lethal effect becomes manifest. Lethally hit cells are assumed to enter a rudimentary cell cycle before ultimately dying.

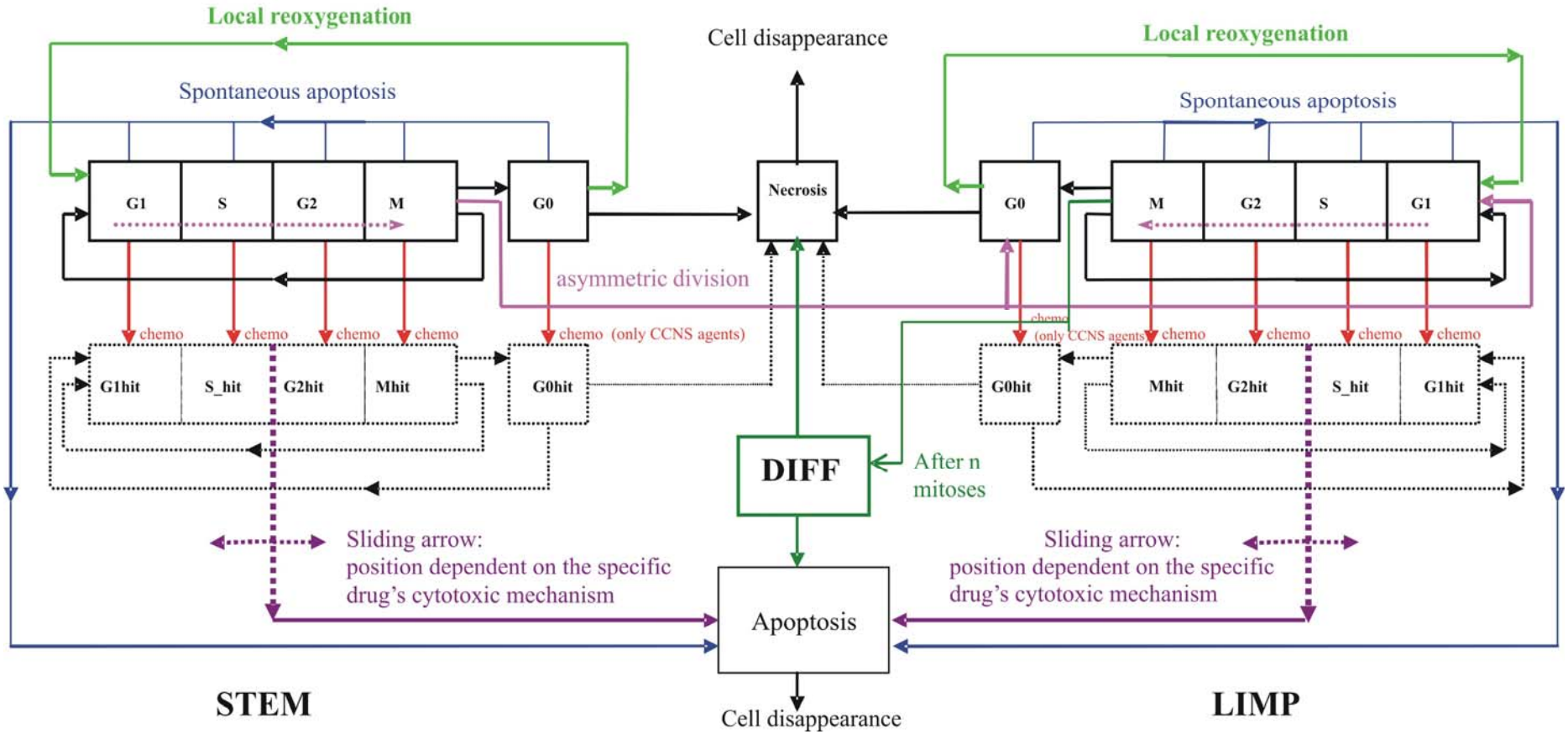

Fig. 4. General cytokinetic model incorporating chemotherapeutic treatment. STEM: stem cells. LIMP: Limited proliferative potential cells. DIFF: terminally differentiated cells. CCNS: cell cycle – nonspecific chemotherapeutic agent. In the present version of the code n has been taken equal to 3. In future versions higher values of n will be explored.

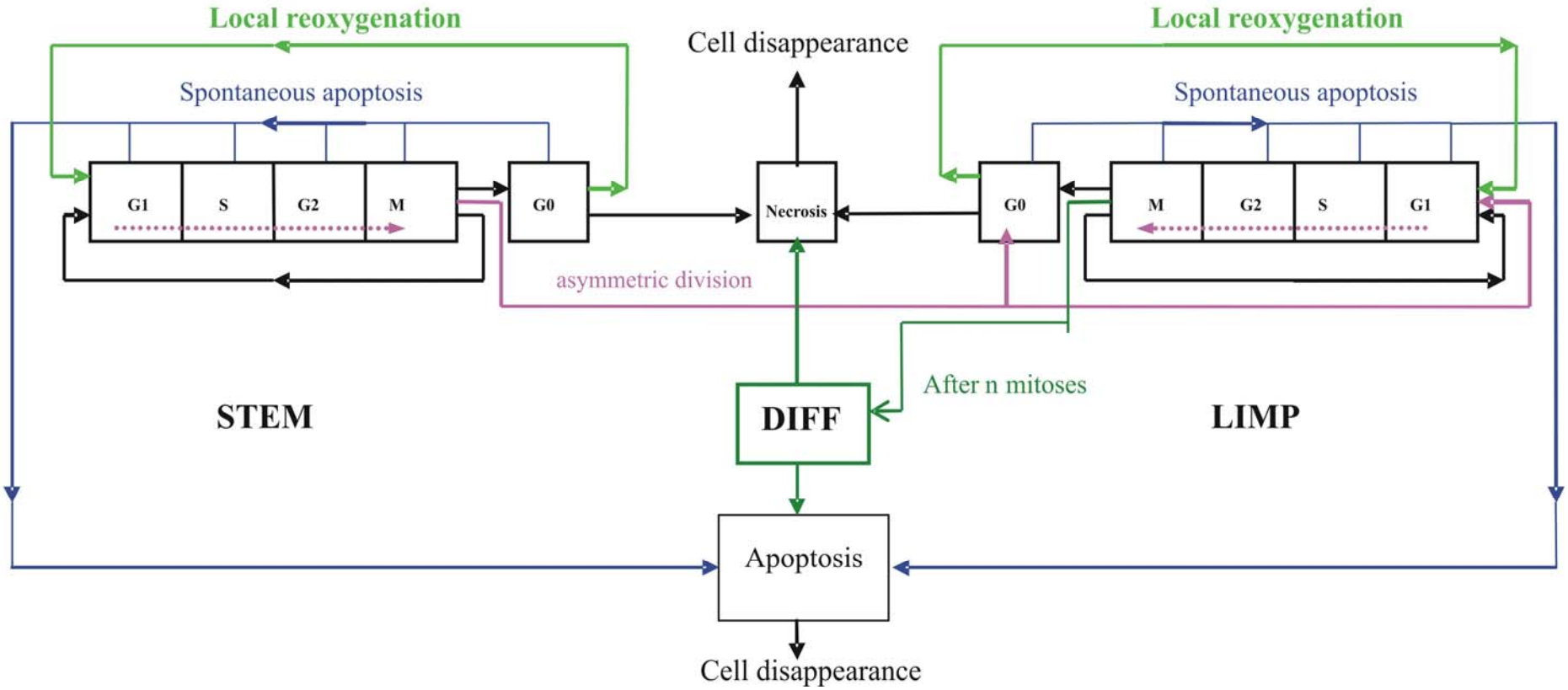

Fig. 5. General cytokinetic model for untreated tumour growth. STEM: stem cells. LIMP: Limited proliferative potential cells. DIFF: terminally differentiated cells. In the present version of the code n has been taken equal to 3. In future versions higher values of n will be explored.

Distribution of the initial number of cells in the basic populations of stem, limp, diff and dead cells.

The discrete character of the simulation model enables the consideration of various exploratory initial percentages of the cells in the various equivalence classes. For future simulations the initialization procedure will be performed based on available clinical data and clinical experience.

Nevertheless, a thorough study of the correlation between initial cell class percentages and values for transition probabilities in the cytokinetic model has been performed. See below the "Nomogram of cell state category transition probabilities and distribution of cell state categories in a free growing tumour" (in Section 7).

It should be reminded that in the current version of the simulation models the tumours are assumed to be spatially uniform and all GCs are initialized in the same way, but in future versions of the models, GCs belonging to different regions of the tumour could be characterized by distinct initial percentages of the various cell populations, as it would be dictated for example from imaging and/or other clinical data.

Algorithms for tumour expansion and shrinkage

In order to simulate tumour expansion or shrinkage, an upper (NBC_{upper}) and a lower limit (NBC_{lower}) in the number of cells in each GC are defined:

$NBC_{upper} = NBC + fr(NBC)$

$NBC_{lower} = NBC - fr(NBC)$

where fr(NBC) represents a fraction of NBC.

At each mesh scan, if the number of tumour cells contained within a given GC becomes less than NBC_{lower}, then a procedure that attempts to "unload" the cells in the neighbouring GCs with less than NBC cells takes place, aiming at emptying the current GC (an 26-GC neighborhood is considered). The unloaded cells are preferentially placed into the neighbouring GCs having the maximum available free space. If two or more of the neihgbouring GCs possess the same amount of free space, then a random number generator is used for the selection. If the given GC becomes empty, it is "removed" from the tumour: An appropriate shift of a chain of GCs, intended to fill the "vacuum", leads to tumour shrinkage. This can happen e.g. after a number of cells have been killed by irradiation.

On the other hand, if the number of cells within a given GC exceeds NBCupper, then a similar procedure attempting to unload the excess cells in the surrounding GCs takes place. If the unloading procedure fails to reduce the number of cells to less than NBC_{upper}, then a new GC "emerges". Its position relative to the "mother" GC is determined using a random number generator. An appropriate shifting of a chain of adjacent GCs leads to the expansion of the tumour. The "newborn" GC contains the excess cells, which are distributed in the various phase classes according to the distribution in the "mother" GC.

As noted above, in the tumour expansion and shrinkage algorithms an appropriate shifting of the contents of a chain of adjacent GCs takes place when a new GC is "created" or an empty GC is "removed" from the mesh. Shifting takes place along lines of random direction. This algorithm is based on the generation of random points on the surface of a hypothetical sphere centered on the GC under consideration. The

shifting of the GCs takes place along the "line" connecting the GC under consideration and the selected random point. The discrete approximation of the line connecting the two points is computed by truncation to the nearest integer. In addition, a special morphological rule is applied; in the case of tumour shrinkage, the outermost (non-empty) GC is detected along each one of among a number of lines of random direction directions of shrinkage. Its "6-Neighbour" GCs belonging to the Tumour (NGCT) are counted. The direction corresponding to the minimum NGCT is selected as the shifting direction. A similar, though inverse, morphological-mechanical rule can be applied in the case of tumour expansion. These morphological rules lead to tumour shrinkage or expansion conformal to the initial shape of the tumour, provided that the mechanical properties of the surrounding normal tissues are assumed to be uniform. The need for the formulation of these morphological rules for tumour shrinkage and expansion has arisen from the inspection of the macroscopic results of the simulation algorithms. A completely random selection of one out of a number of shifting directions results in a premature extensive fragmentation of the tumour region in the case of chemotherapy, which is usually incompatible with clinical experience.

It should also be noted that the value of fr(NBC) influences the uniformity of the mesh in terms of cell density, with a direct impact on the geometrical and volumetric aspects of the simulation. In the current version of the models fr(NBC) = NBC/10. In any case, it should be noted that the underlying biology of the tumour cells remains relatively unaffected by the choice of fr(NBC).

Simulation outline

At each time step the geometrical mesh is scanned and the new "state" of a given GC is determined as follows:

- The time registers of all GCs decrease by one hour.
- Cell loss due to apoptosis and necrosis is computed.
- At time points corresponding to chemotherapy treatment, the number of cells lethally hit is computed based on the survival fraction that has been estimated by the simulation of the specific drugs' pharmacokinetics-pharmacodynamics as described in previous paragraphs. These cells enter the rudimentary cell cycle of chemotherapy-hit cells (Fig. 4).
- Necessary cell cycle phase transitions according to the cytokinetic model are performed.
- Necessary cell transfer between GCs takes place, new GCs are created or empty GCs are deleted according to the tumour expansion/shrinkage algorithms described above. In all cases of cell transfer between GCs an adjustment of the time registers of each class takes place, based on appropriate weighting according to the size of the class populations involved.

DEMONSTRATION OF A POSSIBLE SIMPLE MOLECULAR NETWORK TO REPRESENT THE EFFECT OF MOLECULAR PROFILE TO THE PHARMACODYNAMICS OF EPIRUBICIN WITHIN THE CONTEXT OF THE TOP TRIAL

In the present section a *novel* simplified initial molecular network making use of Boolean algebra logical gates is proposed in order to demonstrate how expressions of key genes in a particular clinical trial can be used in order to adapt the pharmacodynamics of a drug about its population based mean value. Although the exact joint effect of the genes considered may well be modified according to the *details and outcome of the TOP trial*, only for reasons of demonstration, information published in *S.H.Giordano, "Update on Locally Advanced Breast Cancer," The Oncologist, vol.8, pp.521-530, 2003* has been used. According to this paper "For patients treated with anthracycline-based induction chemotherapy, small tumour size, high nuclear grade, high proliferation index (Ki67), and coexpression of HER-2/neu and topoisomerase II have been associated with greater response rates [internal paper references 53–58]. Conversely, mutation of the p53 gene is associated with a lower response rate to chemotherapy [internal papers references 59, 60]. As a first approximation "digitizing" the previous information into "significant" and "non significant" expression levels corresponding to the Boolean values of "1" and "0" respectively we construct the following Boolean molecular network diagram.

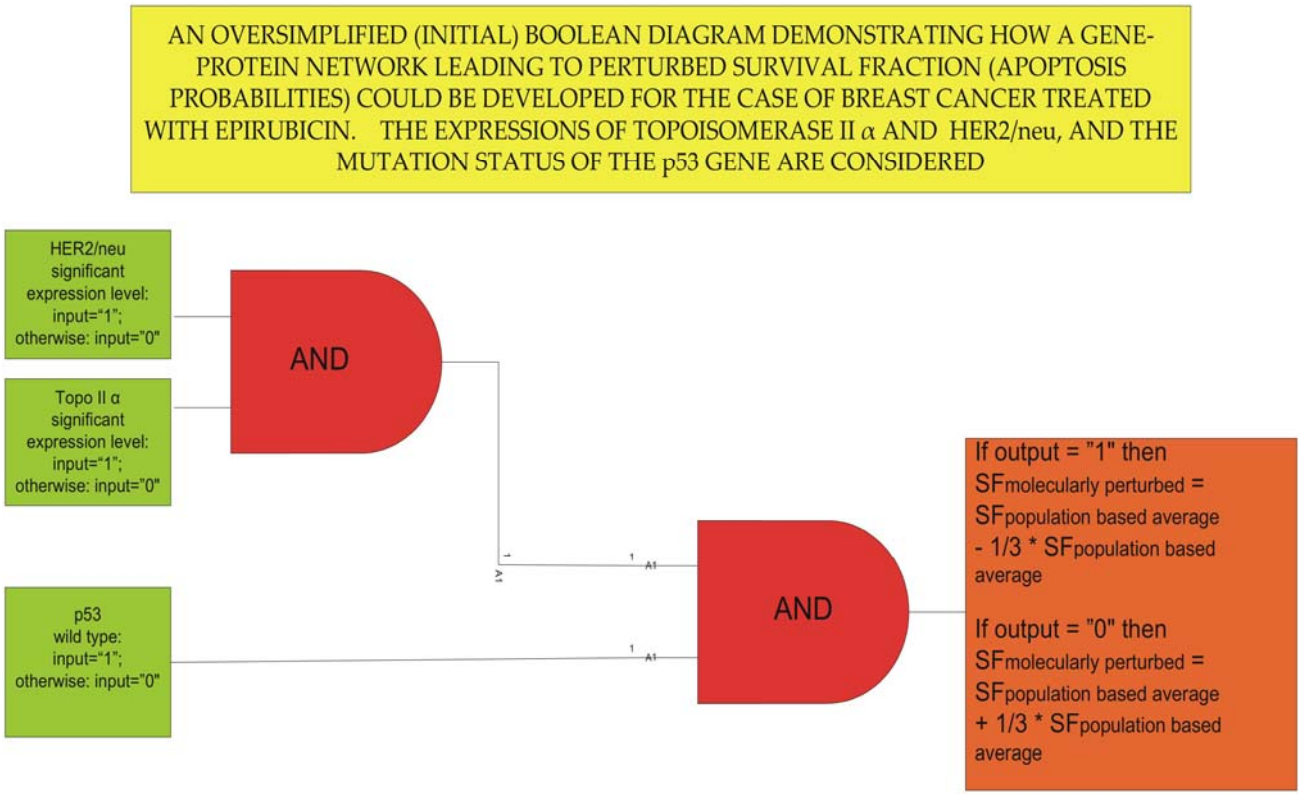

Fig. 6 Obviously the proposed method may serve as a gross first approximation to the incorporation of real molecular data to the multilevel tumour growth and response model developed within the framework of Workpackage 8. SF: survival fraction of tumour cells after each drug dose.

CONSIDERATION OF THE NORMAL TISSUE TOXICITY LIMITS

Before proceeding to the *in silico* experimentation with new chemotherapeutic schedules the toxicity limits for the drug or drugs considered will have to be seriously taken into account in order not to surpass them. Clinical trial phase I data pertaining to the drugs or combinations of drugs considered will serve as valuable sources of such information necessary for the eventual clinical translation of the Oncosimulator.

5 Mathematical Concepts and Methods

The following list contains the major mathematical methods and approaches recruited or developed and applied for the development of the models:

- Differential equation techniques (primarily applied in pharmacokinetics)
- Non deterministic cellular automata
- The generic Monte Carlo technique
- Boolean algebra and logical circuit theory (for the representation of molecular networks)
- A large number of *novel* algorithms specially developed in order to simulate several fundamental biological mechanisms pertaining to many biocomplexity levels.

Throughout the development of the models the concept of the “nomogram of cell state category transition probabilities and distribution of cell state categories in a free growing tumour” as explained in Section 7 has emerged.

6 An Overview of the Simulation Code

CODE INPUT

A - NEPHROBLASTOMA VERSION

In the present initial version of the code the input data are embedded within the code. The following table shows the parameters involved and the values they were given in order to produce the simulation results shown in section 7A.

TABLE 3A INPUT PARAMETER VALUES CORRESPONDING TO THE RESULTS DEPICTED IN FIGURES 9A-17A

//Time durations(hrs)	**Comments**
// Cell-cycle duration	
const int cell_cycle_duration=23;	//Duration of the cell-cycle for nephroblastoma tumours
//Phases duration	
const int max_g1_time=9;	//Duration of phase g1
const int max_s_time=9;	//Duration of phase s
const int max_g2_time4;	//Duration of phase g2
const int max_m_time=1;	//Duration of phase m
// g0	
const int max_g0_time=96;	//Duration of g0 phase 96h
//Dead	
const int necrosis_time=20;	//For how many hours the products of necrosis will occupy space in GM
const int apoptosis_time=6;	//For how many hours the products of apoptosis will occupy space in GM

TABLE 3A (cont.) INPUT PARAMETER VALUES CORRESPONDING TO THE RESULTS DEPICTED IN FIGURES 9A-17A

//Percentages of NBC @ each class

//Percentages of stem-limp-diff-dead

```
const double stem_percent=0.08;

const double limp_percent=0.13;

const double diff_percent=0.75;

const double dead_percent=1.0-(diff_percent+limp_percent+stem_percent);
```

//LIMP percentages

```
const double limp1_percent=0.5;

const double limp2_percent=0.3;

const double limp3_percent=0.2;
```

//percentage of g0 out of prolif and g0

```
const double g0_percent=0.53;
```

//percentages of g1-s-g2-m out of total prolif

```
const double g1_percent=(max_g1_time/cell_cycle_duration)*(1.0-g0_percent);

const double s_percent=(max_s_time/cell_cycle_duration)*(1.0-g0_percent);

const double g2_percent=(max_g2_time/cell_cycle_duration)*(1.0-g0_percent);
```

TABLE 3A (cont.) INPUT PARAMETER VALUES CORRESPONDING TO THE RESULTS DEPICTED IN FIGURES 9A-17A

	const double m_percent=(max_m_time/cell_cycle_duration)*(1.0-g0_percent);	
//Percentages of apoptotic & necrotic		
	const double n_percent=0.88;	
	const double a_percent=0.12;	
//Rates of transitions		
	const double apoptosis_rate=0.001 ;	//spontaneous apoptosis from G1, S, G2,M. G0
	const double diff_nec_rate=0.001;//necrosis of differentiated cells	//apoptosis of differentiated cells
	const double margin_percent=0.10;	//margin of cell population per GC
	const double sleep_percent=0.28;	//M->G0 //percentage of cells that will enter G0
	const double g0_to_g1_percent=0.01;	// G0->G1: how many cells re-enter cell-cycle
	const double sym_percent=0.45;	//Percentage of stem cells that are divided symmetrical
	const double a_loss_rate=0.166;	
	const double n_loss_rate=0.05;	

TABLE 3A (cont.) INPUT PARAMETER VALUES CORRESPONDING TO THE RESULTS DEPICTED IN FIGURES 9A-17A

//Dimensions of the GM (number of GC)

```
const int x_dim=100;
const int y_dim=100;
const int z_dim=100;
```

//cell density= number of biological cells per GC

```
const int number_biological_cells=1000000;   //no of cells per geometrical cell(each GC occupies space of 1mm^3)
```

// max-min number of cells/GC

```
const int max_population_accepted=(int)((1.0+margin_percent)*number_biological_cells);
const int min_population_accepted=(int)((1.0-margin_percent)*number_biological_cells);
```

//Tumour initialisation **Defined in main!!**

```
extern double a;   //length
extern double b;   //breadth
extern double c;   //width
```

TABLE 3A (cont.) INPUT PARAMETER VALUES CORRESPONDING TO THE RESULTS DEPICTED IN FIGURES 9A-17A

//Therapy Scheme: alla time variables in hours!!		**Defined in main!!**
	//which drug to be administered:1.Vincristine, 2.Dactinomycin 3. Combination:vcr+act	
	extern int drug;	
//vcr		
	extern int vcr_adm_interval;	//time interval between 2 administrations
	extern int vcr_start_time;	// How many hours after initializing tumour will the specific drug be administered
	extern int vcr_no_sessions;	//number of sessions of the same drug
	extern double vcr_dose;	//dose per session
	//float vcr_survival_factor;	
	const float vcr_cell_kill_ratio=0.3f;	
//act		
	extern int act_adm_interval;	//dose per session
	extern int act_start_time;	// How many hours after initializing tumour will the specific drug be administered
	extern int act_no_sessions;	//number of sessions of the same drug

TABLE 3A (cont.) INPUT PARAMETER VALUES CORRESPONDING TO THE RESULTS DEPICTED IN FIGURES 9A-17A

```
extern double act_dose;                                          //dose per session
//float act_survival_factor;
const float act_cell_kill_ratio=0.20f;
```

//vcr+act

```
const float combi_cell_kill_ratio=act_cell_kill_ratio+vcr_cell_kill_ratio;
```

//Output files

```
extern const char * file1 ;
extern const char * file2 ;
extern const char * file0 ;
```

TABLE 3A (cont.) INPUT PARAMETER VALUES CORRESPONDING TO THE RESULTS DEPICTED IN FIGURES 9A-17A

INPUT PARAMETER VALUES DEFINED IN MAIN

//vcr		Input in main()
	int vcr_adm_interval;	vcr_adm_interval=168;
	int vcr_start_time;	vcr_start_time=0;
	int vcr_no_sessions;	vcr_no_sessions=4;
	double vcr_dose;	vcr_dose=1.5;
//act		
	int act_adm_interval;	act_adm_interval=336.0;
	int act_start_time;	act_start_time=0;
	int act_no_sessions;	act_no_sessions=2;
	double act_dose;	act_dose=45.0;
//ellipsoid axes		
	double a;	a=10;
	double b;	b=20;
	double c;	c=30;
//drug choice		External input:

TABLE 3A (cont.) INPUT PARAMETER VALUES CORRESPONDING TO THE RESULTS DEPICTED IN FIGURES 9A-17A

int drug;	3
//Interfaces to write data to files as output streams	
ofstream *data2;	//(file1): temporal evolution of populations
ofstream *data;	//(file2): (x,y,z,total_population) spatial distribution of occupied geometrical cells (tumour cells) after therapy
ofstream *data0;	//(file0): (x,y,z,total_population) spatial distribution of occupied geometrical cells (tumour cells) before therapy

B - BREAST CANCER VERSION

In the present initial version of the code the input data are embedded within the code. The following table shows the parameters involved and the values they were given in order to produce the simulation results shown in section 7B.

TABLE 3B INPUT PARAMETER VALUES CORRESPONDING TO THE RESULTS DEPICTED IN FIGURES 9B-16B

//Time durations(hrs)

```
//STEM Cell-cycle duration
const int stem_cell_cycle_duration=23;
const int stem_max_g1_time=int (9.0/22.0*(stem_cell_cycle_duration-1.0)+0.5);
const int stem_max_s_time=int (9.0/22.0*(stem_cell_cycle_duration-1.0)+0.5);
const int stem_max_g2_time=int (4.0/22.0*(stem_cell_cycle_duration-1.0)+0.5);
const int stem_max_m_time=1;

//LIMP Cell-cycle duration
const int limp_cell_cycle_duration=23;
const int limp_max_g1_time=int (9.0/22.0*(limp_cell_cycle_duration-1.0)+0.5);
const int limp_max_s_time=int (9.0/22.0*(limp_cell_cycle_duration-1.0)+0.5);
const int limp_max_g2_time=int (4.0/22.0*(limp_cell_cycle_duration-1.0)+0.5);
const int limp_max_m_time=1;

// g0
```

TABLE 3B (cont.) INPUT PARAMETER VALUES CORRESPONDING TO THE RESULTS DEPICTED IN FIGURES 9B-16B

```
const int max_g0_time=96;

////Dead

const int necrosis_time=20;

const int apoptosis_time=6;


//Percentages of NBC @ each class

//Percentages of stem-limp-diff-dead

                                                                const double stem_percent=0.019;

const double limp_percent=0.077;

const double diff_percent=0.88;

const double dead_percent=1.0-diff_percent-limp_percent-stem_percent;


//percentage of g0 out of total stem or limp

const double g0_percent=0.10;


//percentages of stem g1-s-g2-m out of total stem
```

TABLE 3B (cont.) INPUT PARAMETER VALUES CORRESPONDING TO THE RESULTS DEPICTED IN FIGURES 9B-16B

```
const double stem_g1_percent=(double)stem_max_g1_time/stem_cell_cycle_duration*(1.0-g0_percent);

const double stem_s_percent=(double)stem_max_s_time/stem_cell_cycle_duration*(1.0-
g0_percent);

const double stem_g2_percent=(double)stem_max_g2_time/stem_cell_cycle_duration*(1.0-g0_percent);

const double stem_m_percent=(double)stem_max_m_time/stem_cell_cycle_duration*(1.0-
g0_percent);


//percentages of limp g1-s-g2-m out of total limp

const double limp_g1_percent=(double)limp_max_g1_time/limp_cell_cycle_duration*(1.0-
g0_percent);

const double limp_s_percent=(double)limp_max_s_time/limp_cell_cycle_duration*(1.0-g0_percent);

const double limp_g2_percent=(double)limp_max_g2_time/limp_cell_cycle_duration*(1.0-
g0_percent);

const double limp_m_percent=(double)limp_max_m_time/limp_cell_cycle_duration*(1.0-g0_percent);



//Percentages of apoptotic & necrotic
```

TABLE 3B (cont.) INPUT PARAMETER VALUES CORRESPONDING TO THE RESULTS DEPICTED IN FIGURES 9B-16B

```
const double n_percent=0.8;
const double a_percent=0.2;

//Rates of transitions

const double apoptosis_rate=0.001 ;                                   //spontaneous apoptosis from G1, S, G2,M. G0
const double diff_nec_rate=0.001;//necrosis of differentiated cells
const double diff_apopt_rate=0.001;//apoptosis of differentiated cells
const double n_loss_rate=1.0/necrosis_time; // loss rate of necrotic cells
const double a_loss_rate=1.0/apoptosis_time; //loss rate of apoptotic cells
const double margin_percent=0.10;                                     //margin of cell population per GC
const double sleep_percent=0.10;                                      //M->G0
const double g0_to_g1_percent=0.01;                                   // G0->G1: how many cells re-enter cell-cycle
const double sym_percent=0.14;                                        //Percentage of stem cells that are divided symmetrical
const double stem_div_percent=(1.0+sym_percent)/2.0;//Percentage of stem cells that are derive after symmetric and asymetric divided s
```

TABLE 3B (cont.) INPUT PARAMETER VALUES CORRESPONDING TO THE RESULTS DEPICTED IN FIGURES 9B-16B

```
//Dimensions of the GM (number of GC)
const int x_dim=30;
const int y_dim=30;
const int z_dim=30;

//Dimensions of tumour
const int tumor_length=20;
const int tumor_breadth=20;
const int tumor_width=20;

//cell density= number of biological cells per GC
const int number_biological_cells=1000000;//each cell_bucket occupies space of 1mm^3
```

TABLE 3B (cont.) INPUT PARAMETER VALUES CORRESPONDING TO THE RESULTS DEPICTED IN FIGURES 9B-16B

```
// max-min number of cells/GC

        const int
        max_population_accepted=(1+margin_percent)*number_biological_cells;

        const int min_population_accepted=(1-
        margin_percent)*number_biological_cells;


//Therapy Scheme: time variables in hours!!

        const int week=7*24; //h

        const int adm_interval=3*week;

        const int start_time=0;

        const int no_sessions=4;//number of sessions;

        //const double k=0.85;                                  //Depends on the chemodrug,

        const int dose=100;                                     //per session in mg/m^2
```

THE CORE OF THE CODE

A - NEPHROBLASTOMA VERSION

Table 4A Class wilmstumor UML

Class wilmstumor is the tumor whose growth and response to therapy we simulate. Main variable of this class is an object of class plegma.

wilmstumor_cancer_tumor
mesh:plegma act_stop_time:int vcr_stop_time:int max_stop_time:int stop_time:int
vcr_therapy() act_therapy() combi_therapy()

Class breast_cancer_tumor contains the necessary attributes and functions for the simulation of tumor growth with and without therapy.

Table 5A The attributes of the class are the following:

plegma mesh	the 3D space consists of a mesh of cubic cells.
int act_stop_time	The time @ last administration of act
Int vcr_stop_time	The time @ last administration of vcr
Int max_stop_time	The max stop time between vcr_stop_time and act_stop_time
Int stop_time	Time the simulation stops

Table 6A The functions of the class are the following:

vcr_therapy():	Simulates therapy schemes with vincristine. At administration times, vcr_chemo_action(float vcr_cell_kill) is called. Between administrations, advance_cycle is called per hour.
act_therapy():	Simulates therapy schemes with dactinomycin. At administration times, act_chemo_action(float

	act_cell_kill) is called. Between administrations, advance_cycle is called per hour.
combi_therapy():	Simulates therapy schemes with vincristine and actinomycin. When vincristine is administered, vcr_chemo_action(float vcr_cell_kill) is called. When dactinomycin is administered, act_chemo_action(float act_cell_kill) is called and if vincristine and dactinomycin are administered simultaneously, both function are called. Between administrations, advance_cycle is called per hour.
Grow():	It calls advance_cycle per hour. We call this function in order to simulate free growth of tumour.

B - BREAST CANCER VERSION

Table 4B Class breast_cancer_tumor

breast_cancer_tumor
mesh:plegma survival_factor: float cell_kill_ratio: float drug_concentration: float stop_time: int
epirubicin_pharmacokinetics(in kel:double, k12: double, k21: double, k13: double, k31: double, dose: double, v: double, out auc: double) epirubicin_pharmacodynamics() epirubicin_therapy() grow()

Class breast_cancer_tumor contains the necessary attributes and functions for the simulation of tumor growth with and without therapy.

Table 5B The attributes of the class are the following:

plegma **mesh**	the 3D space consists of a mesh of cubic cells.
float **survival_factor**	percentage of cells not hit by the drug

float **cell_kill_ratio**	percentage of hit cells
int **stop_time**	the stop time (in hours) of the simulation

Table 6B The functions of the class are the following:

double **epirubicin_pharmacokinetics** (double kel,double k12,double k21,double k13,double k31,double dose,double v)	Returns the AUC of the curve drug Concentration=f(t). Input variables are: double **kel** : elimination rate constant double **k12, k21, k13, k31** : intercompartment rate constants double **dose** : chemotherapy drug dose double **v** : volume of distribution
void **epirubicin_pharmacodynamics**()	Computes the cell kill ratio of the drug
void **epirubicin_therapy**()	Simulates the response of the tumor to the chosen therapeutic scheme with epirubicin
void **grow**()	Simulates the free growth of tumor without therapy

OUTPUT FILES

A - NEPHROBLASTOMA VERSION

The code gives as an output three .dat files. :

1. initial_tumour_' system_time'.dat:

Provides the total_population of cells (4rth column) at each occupied geometrical cell @ position x(1rst column), y(2nd column) z(3rd column). It is used for 3D and 2D (planes) visualization of initial tumour volume.

2. final_tumour_'system_time'.dat

Provides the total_population of cells (4rth column) at each occupied geometrical cell @ position x(1rst column), y(2nd column) z(3rd column). It is used for 3D and 2D (planes) visualization of the final tumour volume.

3. tumour_'system_time'.dat:

Provides the time (1rst column) evolution (per h) of three total populations:

- Total proliferating cells(2nd column)
- Total stem cells (3rd column)
- Total cells (4rth column)

B - BREAST CANCER VERSION

The code gives as an output three .dat files. :

1. initial_tumor_'system time'.dat

Represents the initial tumor for 3D or 2D visualization. It contains four columns which correspond to the coordinates of the GCs that belong to the tumor and the number of the total cells that each tumor GC has:

x coordinate - y coordinate - z coordinate - total number of cells of the specific GC

2. final_tumor _'system time'.dat

Represents the final tumor, after the end of the simulation, for 3D or 2D visualization. It contains four columns which correspond to the coordinates of the GCs that belong to the tumor and the number of the total cells that each tumor GC has:

x coordinate - y coordinate - z coordinate - total number of cells of the specific GC

3. tumor_'system time'.dat

Represents the evolution of three characteristic cell populations as a function of time. More specific it contains four columns:

Time (in hours) - total number of tumour stem cells – total number of tumour proliferating cells - total number of tumour proliferating cells – total number of tumour cells

The above files can be opened by Notepad or read by Excel, Matlab etc.

7 Indicative Results

THE NOMOGRAM OF CELL STATE CATEGORY TRANSITION PROBABILITIES AND DISTRIBUTION OF CELL STATE CATEGORIES IN A FREELY GROWING TUMOUR

The initialization of the tumour plays an important role in its time evolution. The initial cell category percentages must be carefully chosen so as to have a tumour that develops smoothly with time without exhibiting any artificial peculiar behaviour at the beginning of the simulation. This is evident in Fig. 7B and Fig. 8B, which correspond to two simulations performed with the same transition percentages and cell cycle durations but with different initial populations of the distinct cell categories (stem, limp, diff and dead cells).

Therefore, a number of exploratory simulation executions have been performed in order to determine the (simulation starting) initial percentages of the various cell category populations that correspond to different transition probabilities and cell cycle durations. The simulations where performed using the parameter values shown in Table 7B. The initial tumour had a diameter of 10mm. Its geometrical cells (GCs) were initialized with 1000 proliferating stem cells each. All other cell category populations were set to zero. The code was executed until 1700h. The rationale behind this approach is that the cell category transition probabilities determine the cell category constitution of a tumour as $t \rightarrow \infty$.

The percentages of the various cell category populations after the end of the execution (1700h) are presented e.g. for the case of breast cancer in the nomogram of Table 8B.

It is noted that in the present initial version of the simulation code each cell of limited mitotic potential (limp or progenitor cell) is assumed to undergo *three mitoses* before it becomes terminally differentiated. The effect of more intermediate mitotic stages will be explored in subsequent versions of the simulation code.

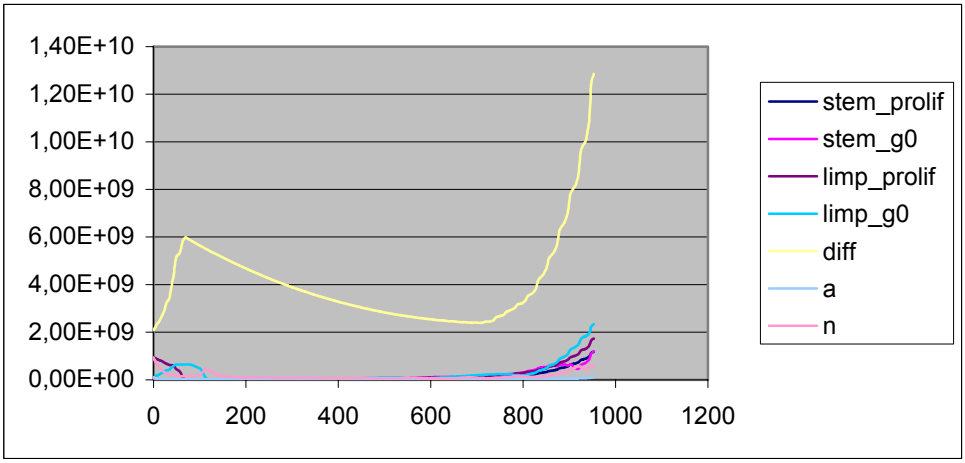

Fig. 7B. Simulation results with inappropriately chosen initial percentages of the various populations in relation to given transition probabilities and cell cycle durations.

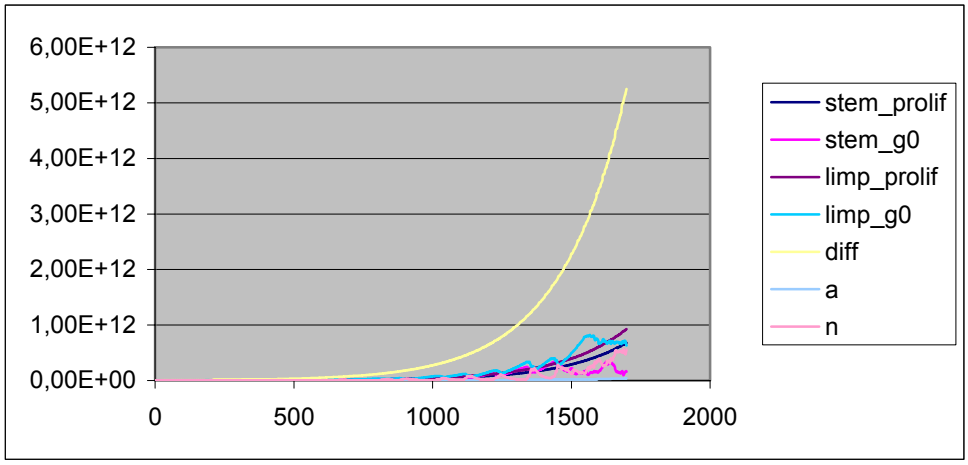

Fig. 8B. Simulation results with appropriately chosen initial percentages of the various populations in relation to given transition probabilities and cell cycle durations.

The following two tables depict the contruction of a nomogram of cell state category transition probabilities and distribution of cell state categories in a freely growing nephroblastoma tumour. Table 7A shows the parameters values used for the production of the nomogram whereas Table 8A presents the nomogram itself.

Table 7A. Parameter values used for the production of the nephroblatoma tumour nomogram

Cell cycle duration =23h	
G0 duration=96h	
apoptosis_rate=0.001	spontaneous apoptosis from G1, S, G2,M. G0
diff_nec_rate=0.001	necrosis of differentiated cells
n_loss_rate=0.05	loss rate of necrotic cells
a_loss_rate=0.166	loss rate of apoptotic cells
margin_percent=0.10	margin of cell population per GC
g0_to_g1_percent=0.01	G0->G1: how many cells re-enter cell-cycle

Table 8A The nephroblastoma tumour nomogram (to be used with Table 7A).										
sleep_percent	prolif_percent	sym_percent	asym_percent	stem_percent %	limp_percent %	Diff_percent %	Dead_percent %	(G0/G0+proli f)%	(Apoptotic/d ead)%	(Necrotic/dead)%
0%	100%	0	1	1	4	93	2	0	21	79
		0,25	0,75	6,5	20	72	1,5	0	29	71
		0,5	0,5	16	35	48	1	0	35	65
		0,75	0,25	34	0	64	2	0	28	72
		1	0	99	0	0	0,5	0	100	0
25%	75%	0	1	2	6	87	5	77	10	90
		0,25	0,75	1	5	91	3	66	15	85
		0,5	0,5	19	25	54	2	63	34	66
		0,75	0,25	51	25	23	1	58	57	43
		1	0	99	0	0	1	0	61	39
50%	50%	0	1	23	7	88	2	86	0	100
		0,25	0,75	5	0	95	0	83	0	0
		0,5	0,5	1	8	91	0	82	0	0
		0,75	0,25	11	13	76	0	89	0	0
		1	0	98	0	0	2	79	0	100
75%	25%	0	1	0	0	0	0	0	0	0
		0,25	0,75	0	0	0	0	0	0	0
		0,5	0,5	0	0	0	0	0	0	0
		0,75	0,25	0	0	0	0	0	0	0
		1	0	100	0	0	0	94	0	0
100%	0%	0	1	0	0	0	0	0	0	0
		0,25	0,75	0	0	0	0	0	0	0
		0,5	0,5	0	0	0	0	0	0	0
		0,75	0,25	0	0	0	0	0	0	0
		1	0	0	0	0	0	0	0	0

NOTICE: Percentages are expressed in the interval between 0 and 100. The rows highlighted in yellow correspond to tumors that self-diminish

The following two tables depict the contruction of a nomogram of cell state category transition probabilities and distribution of cell state categories in a freely growing breast cancer tumour. Table 7B shows the parameters values used for the production of the nomogram whereas Table 8B presents the nomogram itself.

It is noted that the code implementations of the two cases (nephroblastoma and breast cancer) are not identical. This was purposedly done so in order to provide two realtively independent and cross-checkable ways of performing the simulations. Therefore, some parameters and other quantities have been defined in a different but clearly indicated way.

Table 7B. Parameter values used for the production of the breast cancer tumour nomogram

apoptosis_rate=0.001	spontaneous apoptosis from G1, S, G2,M. G0
diff_nec_rate=0.001	necrosis of differentiated cells
diff_apopt_rate=0.001	apoptosis of differentiated cells
n_loss_rate=1.0/20	loss rate of necrotic cells
a_loss_rate=1.0/6	loss rate of apoptotic cells
margin_percent=0.10	margin of cell population per GC
sleep_percent=0.10	M->G0
g0_to_g1_percent=0.01	G0->G1: how many cells re-enter cell-cycle
Cell cycle duration =23h	
G0 duration=96h	

Table 8B The breast cancer nomogram (to be used with Table 7B).										
sleep_percent	**prolif_percent**	**sym_percent**	**asym_percent**	**stem_prolif**	**stem_g0**	**limp_prolif**	**limp_g0**	**diff**	**a**	**n**
		0	1	0,008	0	0,05	0	0,92	0,005	0,017
		0,25	0,75	0,065	0	0,2	0	0,719	0,0047	0,0113
		0,5	0,5	0,212	0	0,292	0	0,484	0,005	0,007
		0,75	0,25	0,504	0	0,248	0	0,241	0,004	0,003
0%	**100%**	1	0	0,995	0	0	0	0	0,005	0
		0	1	0,003	0,007	0,01	0,019	0,9344	0,005	0,02
		0,25	0,75	0,003	0,005	0,015	0,018	0,9213	0,007	0,0307
25%	75%	0,5	0,5	0,0755	0,097	0,1035	0,1073	0,59	0,0047	0,022
		0,75	0,25	0,212	0,296	0,104	0,146	0,233	0,005	0,004
		1	0	0,4978	0,4978	0	0	0	0,0044	0
		0	1	0,000003	0,00007	0,000012	7,28429E-05	0,9756	0,0049	0,019
		0,25	0,75	0,000002	0,00001	0,00000018	0,0000014	0,976	0,0049	0,019
50%	50%	0,5	0,5	0,0000007	0,000014	8,00E-06	0,000036	0,976041	0,0049	0,019
		0,75	0,25	0,0003	0,0014	0,00016	0,0008	0,97244	0,0049	0,02
		1	0	0,173	0,763	0	0	0	0,004	0,06
		0	1	0	0	0	0	0,976	0,005	0,019
		0,25	0,75	0	0	0	0	0,976	0,004	0,02
75%	25%	0,5	0,5	0	0	0	0	0,975	0,005	0,02
		0,75	0,25	0	0	0	0	0,976	0,005	0,019
		1	0	0,04	0,58	0	0	0	0,08	0,3
		0	1	0	0	0	0	0,337	0,121	0,542
		0,25	0,75	0	0	0	0	0,7	0,05	0,25
100%	0%	0,5	0,5	0	0	0	0	0,56	0,08	0,36
		0,75	0,25	0	0	0	0	0,195	0,146	0,659
		1	0	0	0	0	0	0	0,18	0,82

NOTICE: Percentages are expressed in the interval between 0 and 1. The rows highlighted in yellow correspond to tumors that self-diminish

RESULTS

A- THE NEPHROBLASTOMA CASE

Classical graph representation of the results

Free Growth

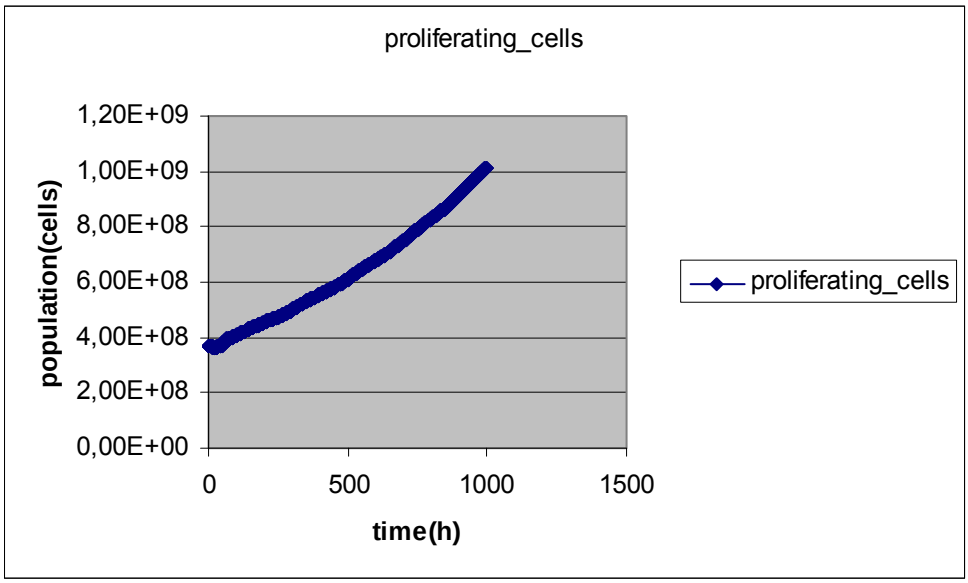

Fig.9A The time course of proliferating cells of a nephroblastoma tumour characterized by the parameter values shown in Table 3A. The time point 0 corresponds to a triaxial ellipsoidal tumour of axes 10 mm, 20mm and 30 mm.

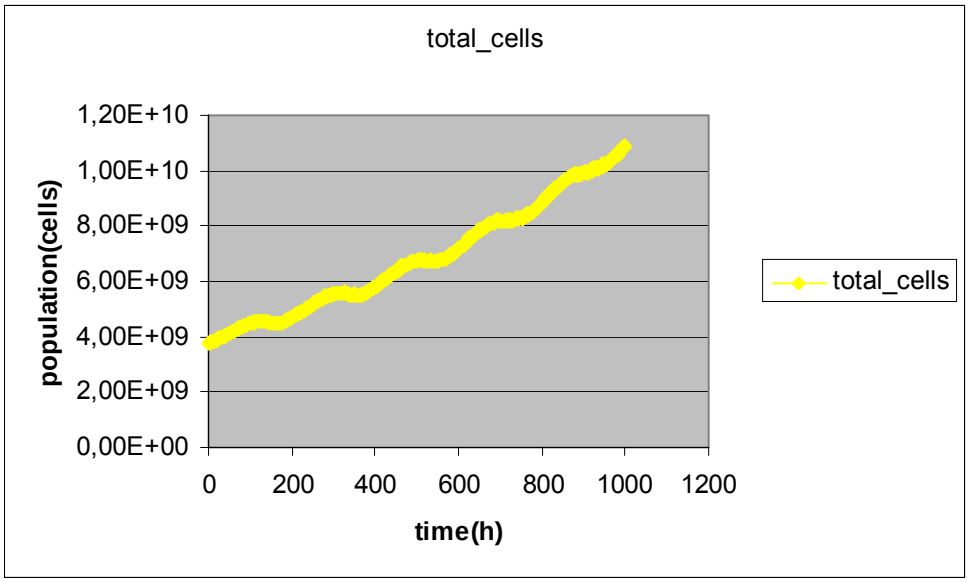

Fig. 10A The time course of the total cells of a wilmstumor characterized by the parameter values shown in Table 3A. The time point 0 corresponds to a triaxial ellipsoidal tumour of axes 10 mm, 20mm and 30 mm.

Response to treatment

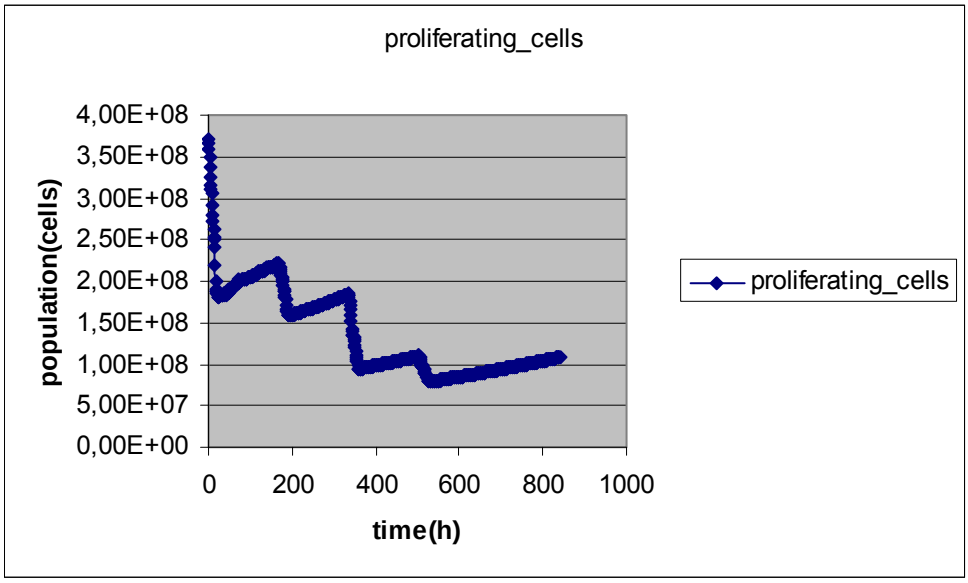

Fig. 11A. The time course of the number of proliferating cells for nephroblastoma tumour treated with vincristine and dactinomycin according to the SIOP 2001/GPOH trial schedule considered in this document. The tumour is characterized by the parameter values shown in Table 3A. The time point 0 corresponds to a triaxial ellipsoidal tumour of axes 10 mm, 20mm and 30 mm. Treatment starts at time t= 0h.

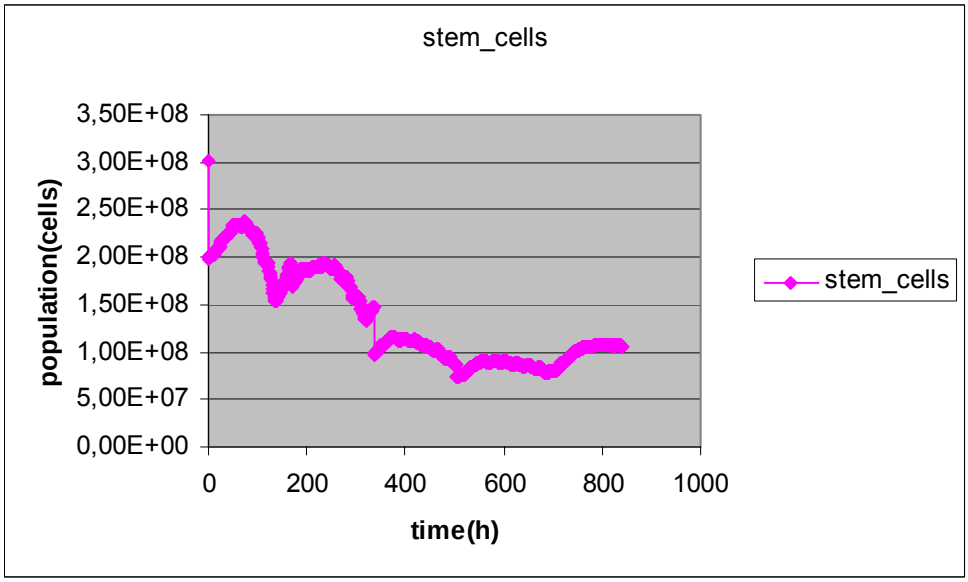

Fig. 12A The time course of the number of stem cells for a nephroblastoma tumour treated with vincristine and dactinomycin according to the SIOP 2001/GPOH trial schedule considered in this document. The tumour is characterized by the parameter values shown in table 3A. The time point 0 corresponds to a triaxial ellipsoidal tumour of axes 10 mm, 20mm and 30 mm. Treatment starts at time t= 0h.

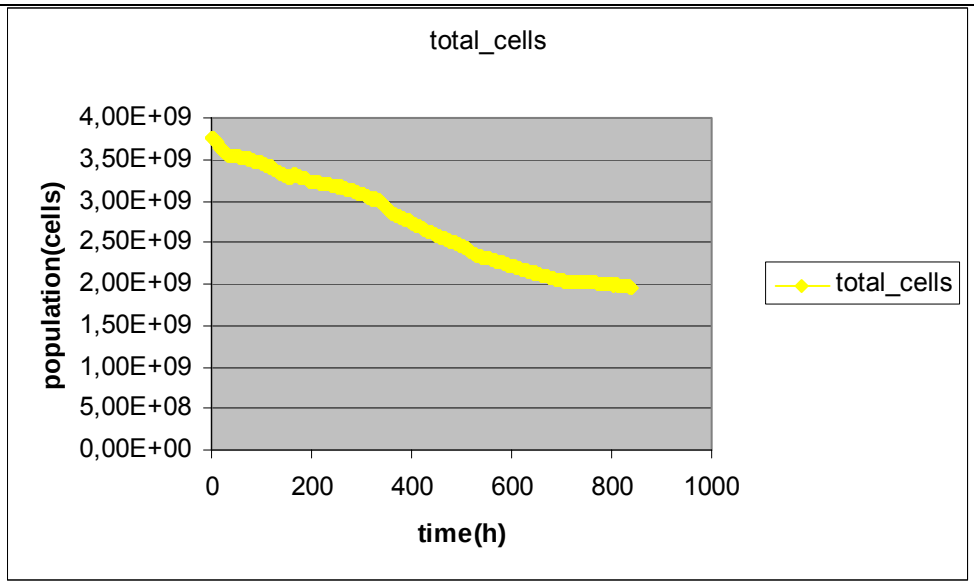

Fig. 13A. The time course of the number of total cells for a nephrobalstoma tumour treated with vincristine and dactinomycin according to the SIOP 2001/GPOH trial schedule considered in this document. The tumour is characterized by the parameter values shown in table 3A. The time point 0 corresponds to a triaxial ellipsoidal tumour of axes 10 mm, 20mm and 30 mm. Treatment starts at time t= 0h.

Simple three dimensional rendering of the results

Response to treatment

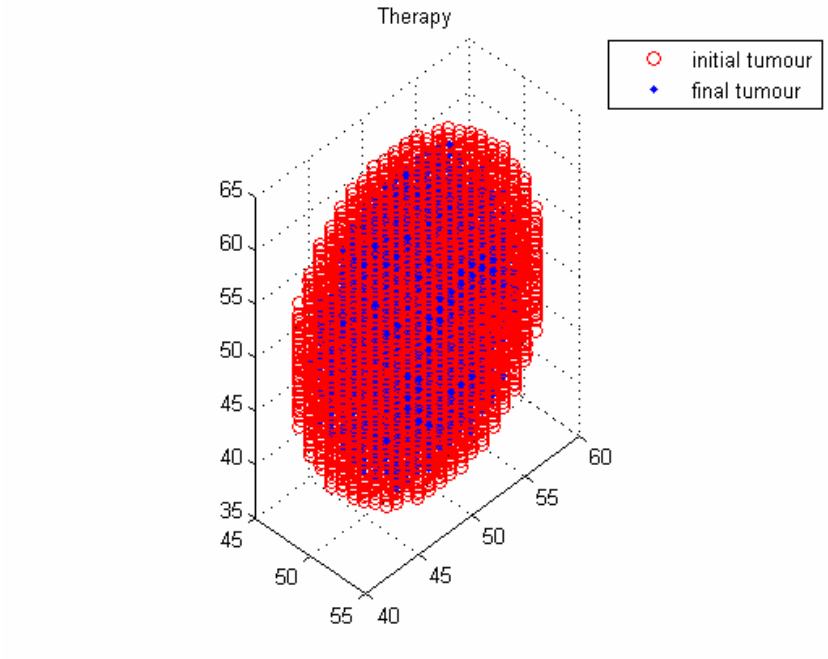

Fig.14A. Simulation results with treatment. The tumour is visualized two weeks after the end of the treatment scheme. The tumour is characterized by the parameter values shown in table 3A. The time point 0 corresponds to a triaxial ellipsoidal tumour of axes 10 mm, 20mm and 30 mm. Treatment starts at time t= 0h.

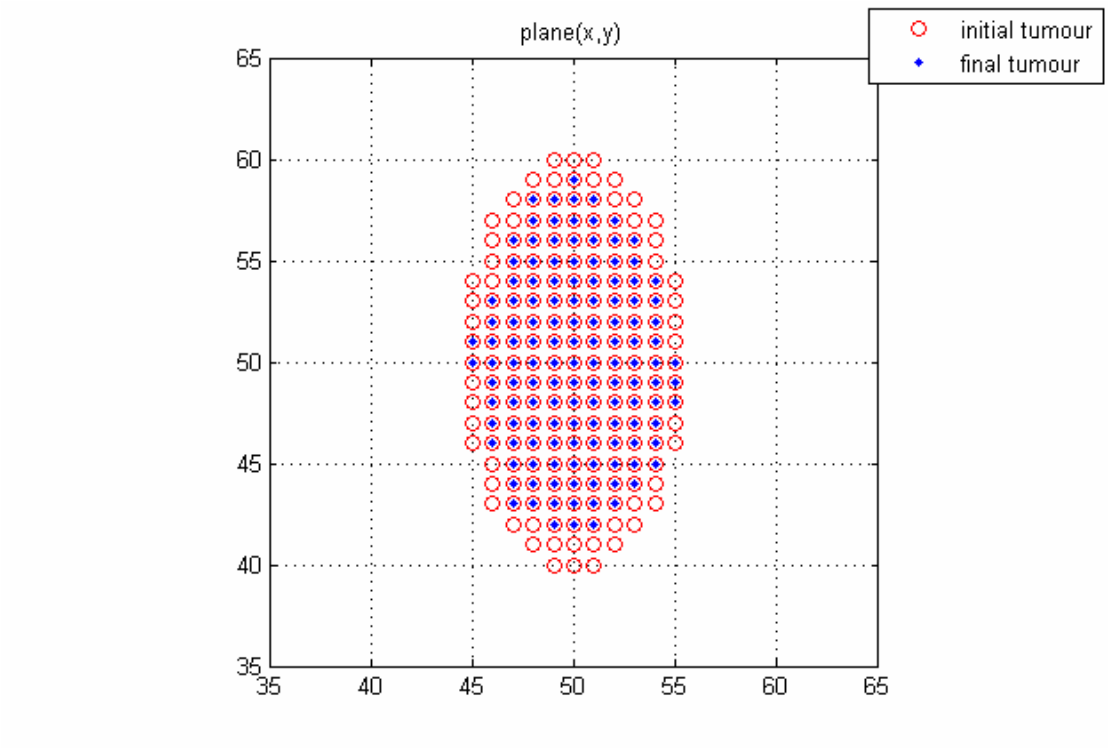

Fig. 15A. Simulation results with treatment. The tumour is visualized two weeks after the end of the treatment scheme. Projection on the xy plane

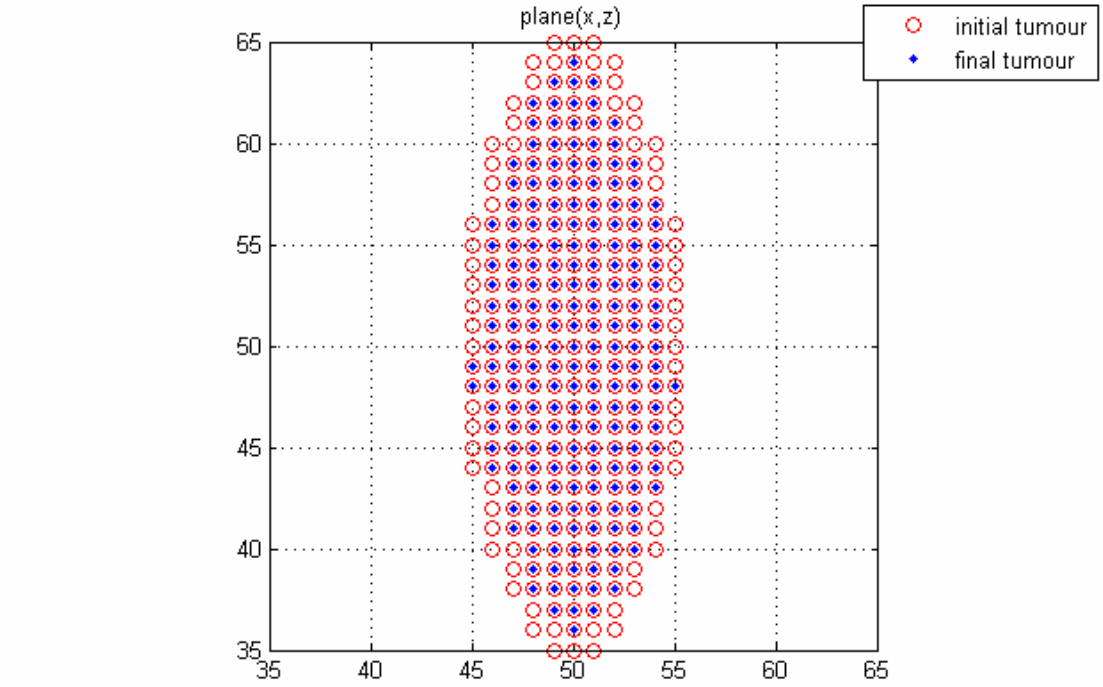

Fig. 16A. Simulation results with treatment. The tumour is visualized two weeks after the end of the treatment scheme. Projection on the xz plane

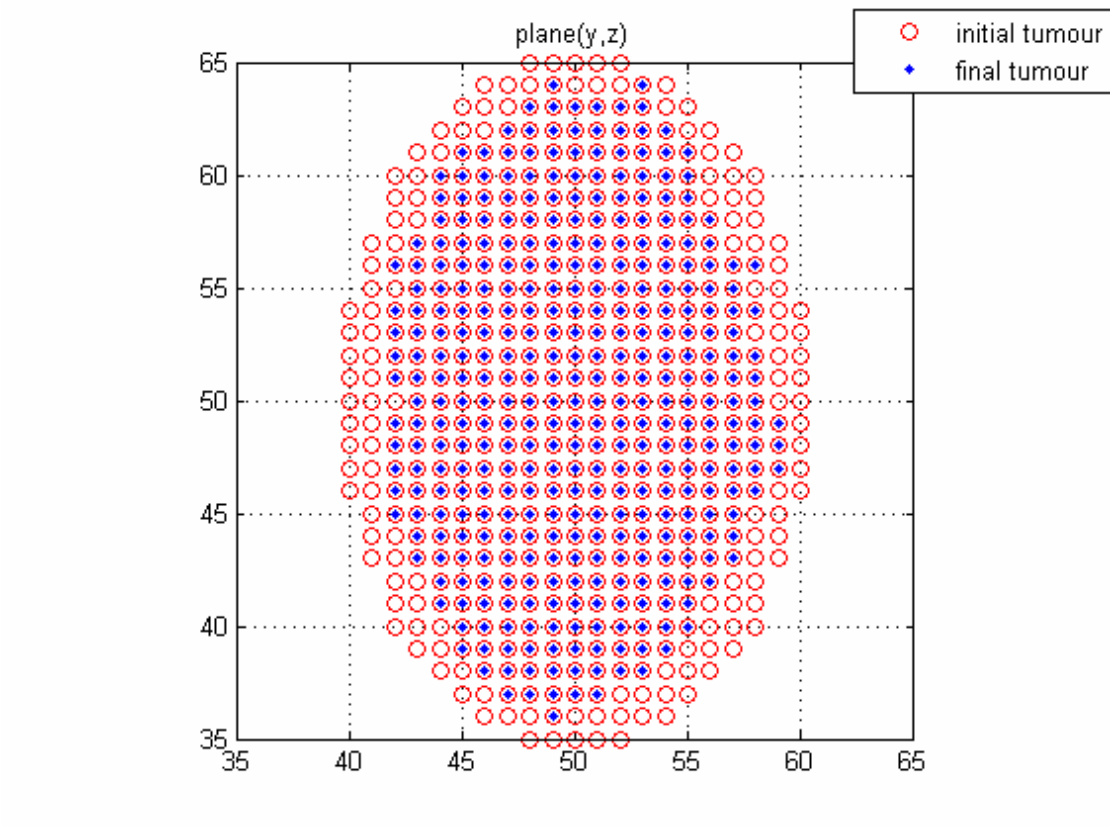

Fig. 17A. Simulation results with treatment. The tumour is visualized two weeks after the end of the treatment scheme. Projection on the yz plane

B - THE BREAST CANCER CASE

Classical graph representation of the results

Free Growth

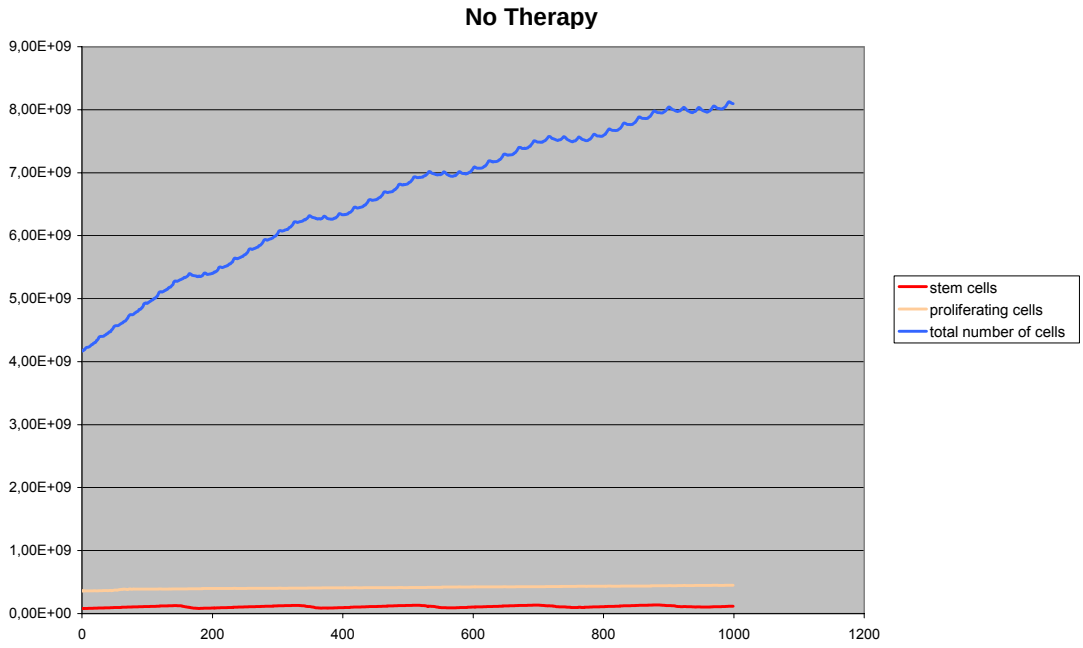

Fig.9B The time course of the number of stem cells, proliferating cells and total number of cells for free growth of a breast tumour characterized by the parameter values shown in Table 3B. The time point 0 corresponds to a diameter of the tumour equal to 2 cm. A Gompertzian increase of tumour volume is obvious.

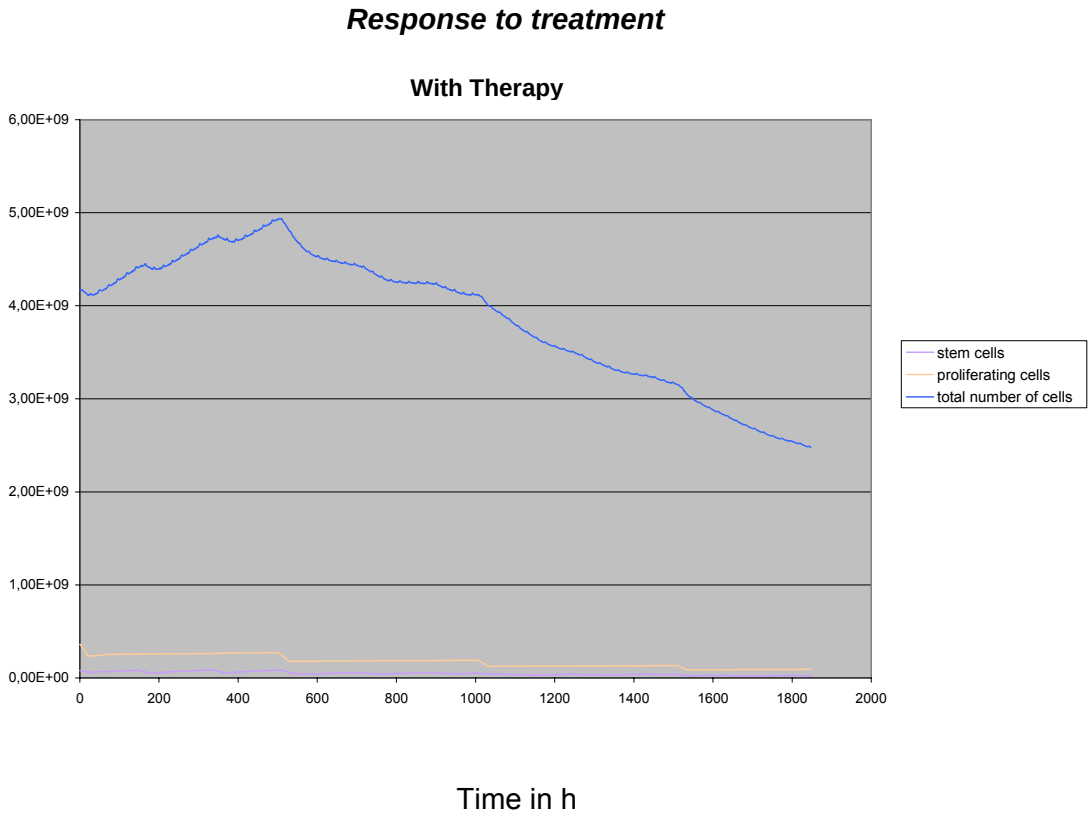

Fig. 10B The time course of the number of stem cells, proliferating cells and total number of cells for a breast tumour treated with epirubicin according to the TOP trial schedule considered in this document. The tumour is characterized by the parameter values shown in Table 3B. The time point 0 corresponds to a diameter of the tumour equal to 2 cm. Ttreatment starts at time = 0h. During the first chemotherapeutic cycle only a decrease of the growth rate of the tumour is noted for the *particular* set of parameters considered. After the second drug administration the tumour shrinkage is more pronounced.

Simple three dimensional rendering of the results

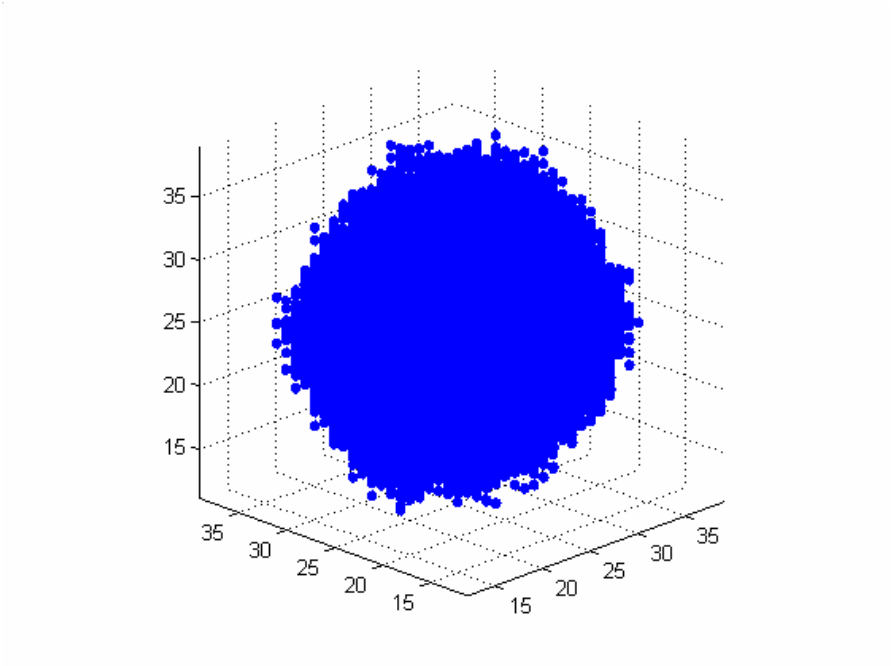

Fig. 11B Breast cancer tumour simulation results with no therapy. The tumour is visualized 42 days after the beginning of the simulation. At the beginning of the simulation the diameter of the tumour was 2 cm.

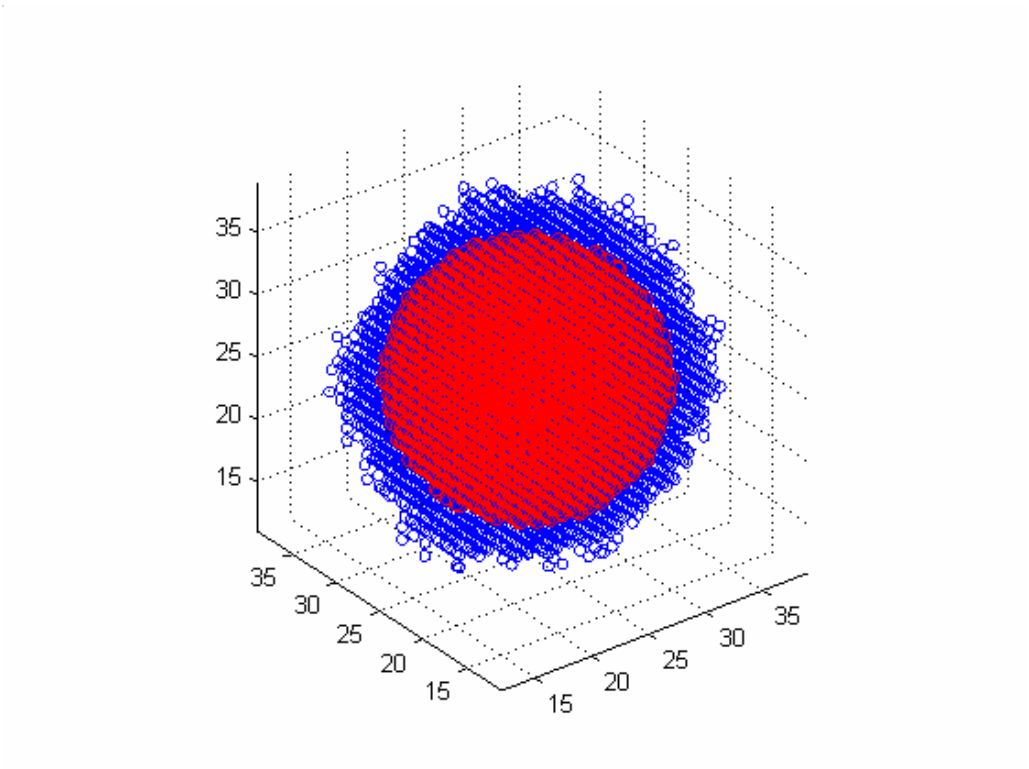

Fig. 12B Breast cancer simulation results with no therapy. The tumor is visualized 42 days after the beginning of simulation. At the beginning of the simulation its diameter was 2 cm. Colour Coding: Red: Initial Tumor. Blue: Tumour after 42 days.

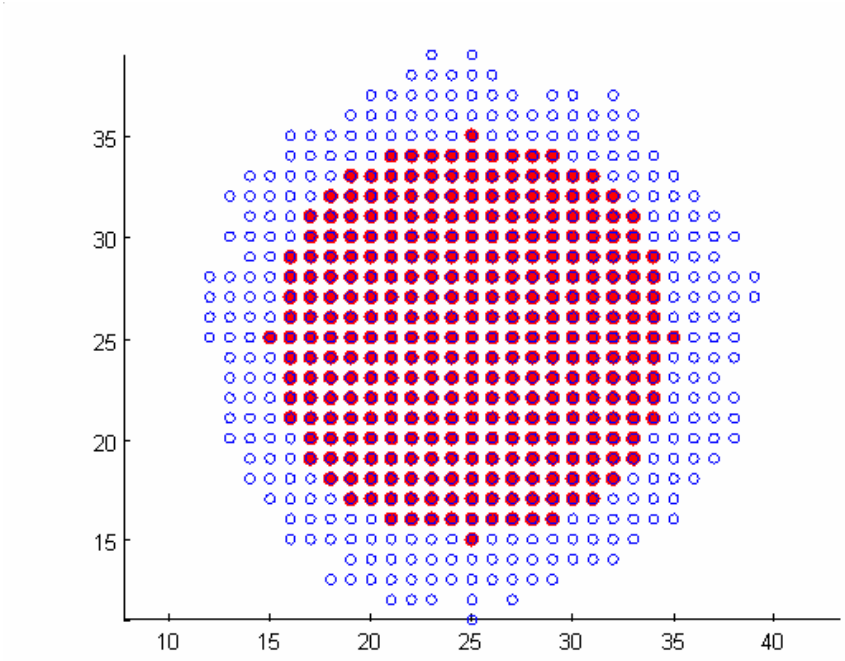

Fig. 13B .Breast cancer simulation results with no therapy. The tumor is visualized 42 days after the beginning of simulation. At the beginning of the simulation its diameter was 2 cm. Colour Coding: Red: Initial Tumour , Blue: Tumour after 42 days. Projection on the xy plane.

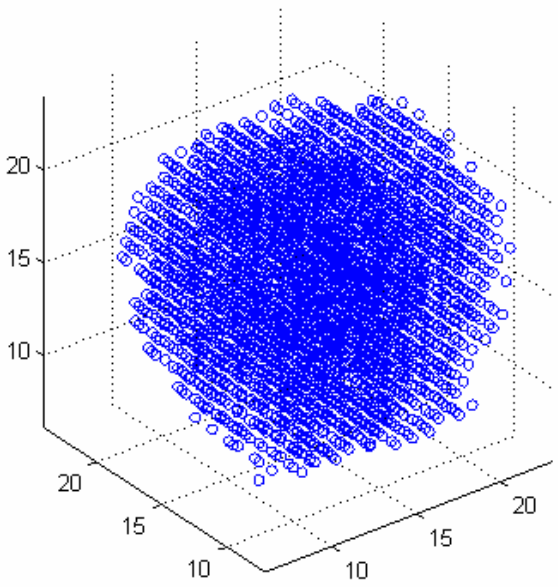

Fig. 14B Simulation results with therapy. Tumour two weeks after the end of the treatment scheme

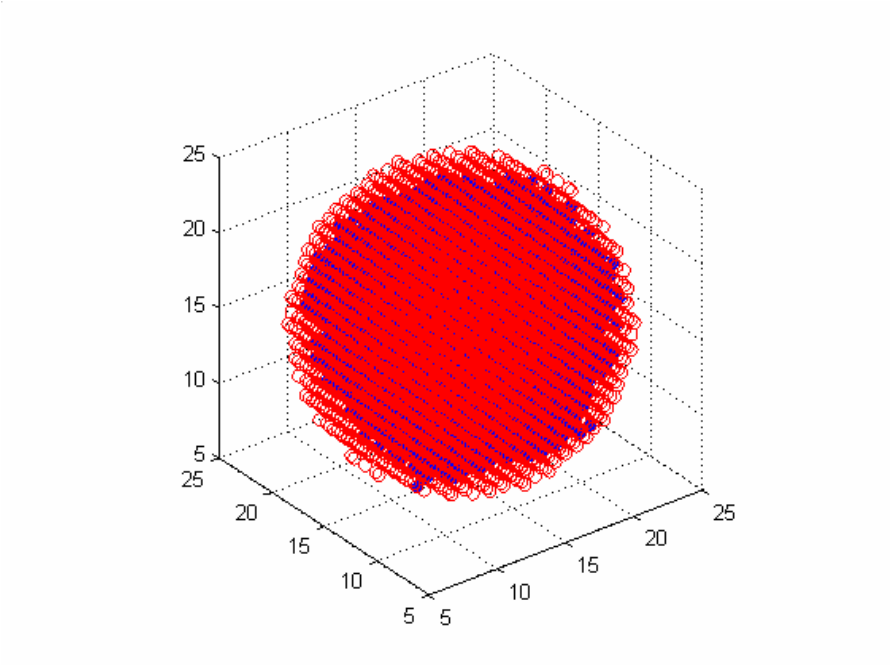

Fig. 15B Simulation results with therapy. The tumor is visualized two weeks after the end of the treatment scheme. Colour Coding: Red: Initial Tumor Blue: Tumour two weeks after the end of the treatment scheme.

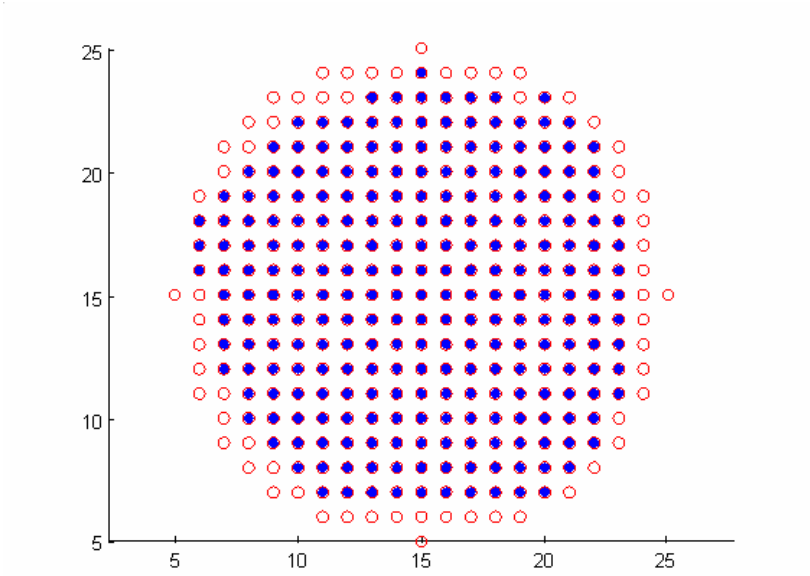

Fig. 16B Simulation results with therapy. The tumor is visualized two weeks after the end of the treatment scheme. Colour Coding: Red: Initial Tumor Blue: Tumour two weeks after the end of the treatment scheme. Projection on xy plane

8 Next Steps

The immediate next steps of the simulation component development will be the following:

- Consideration of clinical (imaging) data for which the triaxial ellispoidal shape seems not to be a good approximation of their boundaries i.e. consideration of tumours with remarkably arbitrary shapes
- Consideration of non macroscopically homogeneous tumours i.e. tumours which show a macroscopic proliferative-necrotic structure based on imaging data
- Consideration of a higher number of mitoses that progenitor (LIMP) cells undertake before they become terminally differentiated tumour cells
- Systematic collection and preprocessing of heterogeneous medical data (imaging, histopathological, molecular and clinical) in order to refine, better adapt and clinically validate the models
- Integration with the technological components with which the simulation component will consitute the ACGT Oncosimulator

9 Conclusion

The present report, although not a complete account of all the details and intricacies of the models developed, has provided an outline of all the major constituent modules, the basic assumptions made, the models' behaviour as well as the points that seem to be amenable to further refinement. The next steps to be taken in order to bring the models closer to the clinical environment, for which they have been *ab initio* designed, have also been outlined. The indicative results presented, being comparable with the clinical reality, support the clinical potential, the flexibility and the robustness of the models.

Concerning especially the *degrees of freedom* of the simulated system to be clinically adapted, it should be born in mind that many parameters appearing in i.e. the cytokinetic diagrams of Fig.4 and Fig.5 are not independent. For example 16 cell cycle phase durations appearing on Fig.4 can be approximately calculated from the values of a *single* parameter e.g. the cell cycle duration. This is feasible since certain cell cycle phases (S phase and mitosis) tend to have the same duration regardless of the whole cell cycle duration whereas the gap (G1 and G2) phases are lengthened in a proportional way so that they make up the rest (non S and non M) cell cycle duration. Simpler interdependence models of cell cycle duration parameters have also appeared in literature and considered during the development of the present models. Furthermore, reasonable population based values of all parameters are assigned so that the clinical data are not to be viewed as the only source of information for the determination of the parameter values appearing in the models but rather as a *means for the refinement* of the initial parameter values based on the individual patient's data. In other words the development and clinical adaptation of the model will be an evolutionary process of which the *refinement* will depend on the available medical (imaging, histopathologic, molecular and clinical) data to be provided by the two clinicogenomic trials originally addressed by ACGT.

Appendix 1 Calculations for epirubicin pharmacokinetics: a three-compartment model

For a three-compartment first order pharmacokinetic model the plasma drug concentration can be given by:

$$C_1 = Ae^{-\alpha t} + Be^{-\beta t} + \Gamma e^{-\gamma t}$$

A physical interpretation for the three-compartment first order model is the consideration of a central compartment, a deep peripheral compartment and a superficial peripheral compartment, as depicted in the following figure:

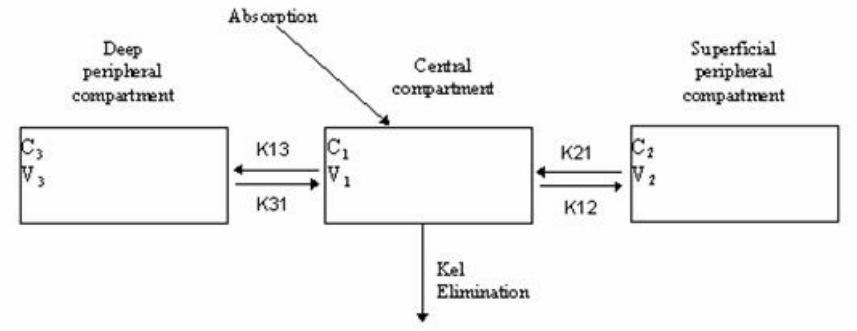

where C_i, V_i are the concentration and volume of each compartment, k_{el} is the elimination rate constant from the central compartment, and k_{12}, k_{21}, k_{13}, k_{31} are the rate constants describing drug transfer between the compartments.

$a = k_{el}+k_{12}+k_{21}+k_{13}+k_{31}$

$b = k_{el}*k_{21}+kel*k_{31}+k_{12}*k_{31}+k_{31}*k_{21}+k_{21}*k_{13}$

$c = k_{el}*k_{21}*k_{31}$

and

$$\phi = \arctan \sqrt{\frac{\left(\left(\frac{a}{3}\right)^2 - \frac{b}{3}\right)^3}{\left(\left(\frac{a}{3}\right)^3 + \frac{c - \frac{a*b}{3}}{2}\right)}} - 1$$

Then the parameters α, β, γ are given by:

$$\alpha = \frac{a}{3} + 2*\sqrt{\left(\frac{a}{3}\right)^2 - \frac{b}{3}} * \cos\left(\frac{\phi}{3}\right)$$

$$b = \frac{a}{3} + 2*\sqrt{\left(\frac{a}{3}\right)^2 - \frac{b}{3}} * \cos\left(\frac{\phi}{3} + \frac{4*\pi}{3}\right)$$

$$\gamma = \frac{a}{3} + 2 * \sqrt{\left(\frac{a}{3}\right)^2 - \frac{b}{3}} * \cos\left(\frac{\phi}{3} + \frac{2*\pi}{3}\right)$$

Therefore,

$$A = \frac{dose}{V_1} \frac{(\alpha - k21) * (\alpha - k31)}{(\alpha - \beta) * (\alpha - \gamma)}$$

$$B = \frac{dose}{V_1} \frac{(\beta - k21) * (\beta - k31)}{(\beta - \alpha) * (\gamma - \alpha)}$$

$$\Gamma = \frac{dose}{V_1} \frac{(\gamma - k21) * (\gamma - k31)}{(\gamma - \beta) * (\gamma - \alpha)}$$

and finally, the area under curve is given by:

$$AUC = \int_{t=0}^{\infty} C dt = \int_{t=0}^{\infty} (Ae^{-at} + Be^{-\beta t} + \Gamma e^{-\gamma t}) dt$$

$$AUC = \frac{A}{a} + \frac{B}{\beta} + \frac{\Gamma}{\gamma}$$

Thus AUC is described as a function of the transfer rate constants, the drug dose and the volume of distribution.

Appendix 2 - Abbreviations and acronyms

ACT	Actinomycin D or Dactinomycin
AUC	Area Under Curve
CR	Complete Remission
ER	Estrogen Receptor
GC	Geometrical Cell
IC_{50}	Drug concentration eliciting 50% of the maximum inhibition
LIMP	LImited Mitotic Potential Cells also known as progenitor cells
NC	No Change

PD	Progressive Disease
PgR	Progesteron Receptor
PR	Partial Remission
VCR	Vincristine
Vd	Volume of Distribution